Downdraft gasifier modeling

Submitted by:

Frank Sebastián Comas Gil
Code: 201010038004
fcomasg@eafit.edu.co

Advisor: Santiago Builes Toro., Ph.D

UNIVERSIDAD EAFIT

SCHOOL OF ENGINEERING

PROCESS ENGINEERING DEPARTMENT

MEDELLIN

2016

Table of Contents

1. Introduction

Gasification is a complex process that integrates a series of transformation phenomena allowing the conversion of carbon rich feedstock, preferably biomass, into a valuable and useful gaseous fuel; essentiality is composed of 4 stages or sub-processes (i.e., drying, pyrolysis, oxidation and reduction). The understanding of its principles and key parameters are essential for the design and operation of gasification equipment [1].

Understanding gasification as a chain of transformations is very important to learn how to operate a gasifier. Mathematical process modeling is used to represent and simulate complex processes such as gasification [2].

Downdraft gasifiers configuration are one of the most commonly used. For the correct operation of this kind of unit, and its proper process control, a complete understanding of the underlying principles of downdraft gasification is required. The subsequent work presents a mathematical model based on literature sources that seeks to overcome the knowledge gap between gasification principles and their effects on a downdraft gasifier operation. Although the results were not fully successful, the model traces the basis to obtain valuable insights about the performance and a more complete understanding of the internals of a downdraft gasifier. The model represents the four stages of gasification with their particular chemistry; it has a unidimensional level and kinetic nature. The model algorithm was solved complete with four stages and two-partial segments of the stages and validated with experimental data. The results obtained in drying and pyrolysis processes were in line with the kinetic quantities expected. Significantly, energy conservative aspects, due to the assumptions taken, were not equivalent to experimental data.

2. Aims and objectives

Aim

To develop and implement a suitable mathematical model for analyzing and evaluating the outcome in the process performance of modifying different operating parameters of downdraft gasifiers.

Objectives

- To determine the most important principles that represent the behavior of a downdraft gasifier and allow the prediction of the process performance with changes on the operating parameters.
- To implement a model for a downdraft gasifier based on literature sources.
- To validate the downdraft gasifier model proposed in order to stablish its accuracy.
- To predict the composition of the gases generated within each stage of a downdraft biomass gasification process.

3. Conceptual framework

3.1. Gasification: an alternative for energy generation

Energy demand is one of the biggest concerns worldwide due to continuous population growth. One of the main options to supply this growing energy demand is through renewable energy sources, which contribute to the decrease the emissions of greenhouse gases. Biomass has a large potential to contribute to the global energy demand due to the large amount of energy that can be released when the bonds of their polymeric structures are broken. According to GENI (Global Energy Network Institute) in 2009, the energy supply by renewable sources in Colombia, excluding hydropower, was 15.2% of the total energy supply. This value highlights the potential for developing different options of renewables in the energy mix in Colombia [1]. In 2010 biomass and biomass derived fuels had a share of 10% in the world's primary energy mix, a low figure taking into account its potential [2].

Basically there are two different routes for biomass conversion. The first one is biochemical conversions, which is the most traditional route, among the biochemical processes for converting biomass to energy are fermentation, digestion and enzymatic hydrolysis. These techniques are widely used nowadays, even though they have some limitations. Although not much external energy is required for those biochemical conversion processes, they are much slower than thermochemical conversion processes. Thermochemical conversion is the second route for biomass conversion, this process of transformation of biomass is more focused in thermal energy production. Moreover, it can be divided, mainly, into four different processes: combustion, pyrolysis, liquefaction and gasification [3].

Combustion is the oldest means to convert biomass into energy, burning wood was the first step of humanity into civilization; combustion is a reaction between oxygen and hydrocarbon in biomass, to obtain H_2O and CO_2; its nature is exothermic [4]. Pyrolysis takes place in the total absence of oxygen; large hydrocarbon molecules of biomass are broken down into smaller molecules. Liquefaction, unlike the processes mentioned before, is a process to generate a liquid fuel from a solid biomass through the presence of water or solvent [3].

Gasification processes allow the use of biomass as feedstock; most of the implementations nowadays are focused on biomass as a primary input [5]. The thermochemical route of gasification has a lower environmental impact than other thermochemical conversion processes, such as combustion, due to its lower CO_2 emissions per Joule [4] .

The main chemical products resulting of gasified biomass are a mixture of gases whose major components are carbon dioxide, carbon monoxide, methane and hydrogen. These gases are used mainly for: (i) heat production or (ii) gas turbine systems, depending on the specific properties of the gas. Recent developments have allowed high selectivity towards

specific gases. For instance, Grammelis et. al. reviewed a branch of techniques to obtain pure hydrogen through selective catalysts, iron-chromium and copper-zinc based catalyst, fostering hydrogen formation and afterwards; separation by pressure swing adsorption. With this technology it is possible to produce high purity hydrogen, up to 99.999 %v [5]. Thereby, gasification has become not only an energy production alternative but also it is a process for chemical feedstocks.

Biomass gasification involves a number of complex thermochemical processes. Independent of the gasifier type, generally the biomass gasification process is divided into four main stages: (I.) drying of biomass, (II.) pyrolysis, (III.) oxidation and (IV.) reduction. *Figure1* depicts a schematic of these stages in a downdraft gasifier [6].

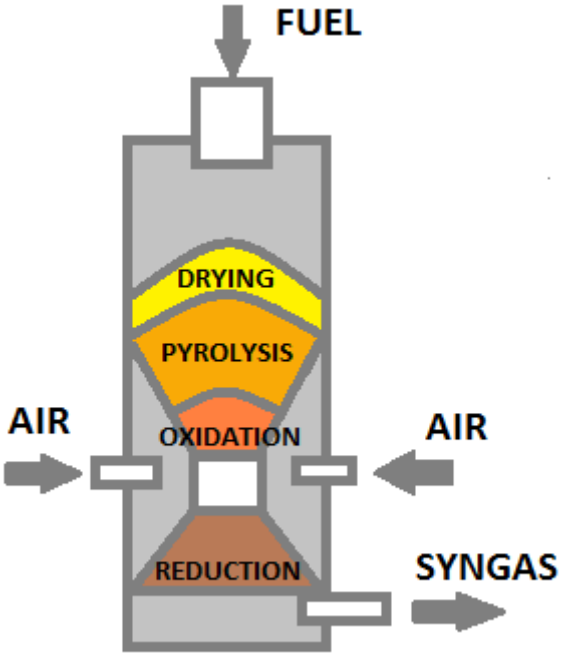

Figure 1. Schematic of a downdraft gasifier. Adapted from Budhathoki **[7]**.

Although these stages are frequently modeled in series, to ease the simulations, there is not a well- defined boundary among them and they often overlap [6].

- **Drying**

  Biomass has an inherent content of moisture. This water needs to be evaporated before continuing the gasification. The energy invested in the water vaporization is not recoverable, which is why moisture content is an important aspect to look at. Ranges of moisture in biomass vary from 30% to 60% [4].

- **Pyrolysis**

  Key step in which biomass is devolatilized. Char, gas, and tars are formed in this stage. Pyrolysis of biomass is typically carried out in a temperature range of 300°C-650°C, which involves a breakdown of large complex molecules into several smaller ones. The gas species are generally a mixture of CO_2, H_2O, CO, C_2H_2, CH_4, H_2, C_2H_6 and C_6H_6. Tars are problematic because they are sticky liquids, difficult to convert into something useful. Char formation is the most important product of this stage and is the input for the reduction stage [4].

- **Oxidation**

  This phenomenon integrates the partial oxidation of pyrolysis products in the presence of the gasification agent. Heterogeneous and homogeneous reactions are present in the stage. Although, the chemistry can vary depending on the model, the basic products are CO_2, CO and H_2 [7] . The char combustion reaction also takes place in the oxidation stage. The importance of the combustion reaction lies on the heat that it produces. Most of the other reactions are endothermic and the char combustion reaction ensures the energy to maintain the process running [4].

- **Reduction**

  The biomass char produced in the pyrolysis stage reacts with the gasifying medium, formed in the previous stages, breaking down the char and making up the final product: syngas [4].

The specific chemistry in each stage of the model is explained in section 5.

3.2. Modeling gasification

Mathematical modeling is a tool that uses preliminary knowledge of the phenomena being modeled to predict the behavior of the system under certain conditions. It is possible to implement a model before performing an experimental procedure, thus allowing to test different outcomes of the process. Moreover, in certain situations modeling allows to understand the behavior of the process under conditions that otherwise might be difficult to reproduce experimentally. Although trial and error tests are often used to improve processes, these methods are costly and more time consuming than process model optimization [8]. Furthermore, a mathematical model representing a process gives more flexibility to face substantial changes in operation, feedstock or equipment [9].

Particularly, for the modeling of gasification of biomass it is important to consider that this process consists of 4 different stages; drying, pyrolysis, oxidation and reduction. Each one of these stages has its particular chemistry and conditions of operation [10]. It is clear that such a process has a high complexity and requires a specific model for each of its stages.

The efficient performance of a gasifier is a challenging task. Gasification modeling allows framing the chemical and physical principles of operation of the equipment and the process. However, the model alone is not enough to ensure the right performance of the process. The model itself is unable to evaluate key parameters autonomously. Modeling an accurate evaluation relies on setting operating parameters that have large influence on the gasification process. The key parameters are cataloged as inputs to the model because are variables to be studied in order to determine optimal points of operation. [10] Key operating parameters are: (i) feedstock flow rate, (ii) gasifying agent flow rate and (iii) initial ignition temperature. However there are other parameters commonly fixed to the feedstock or the specifications of the gasifier, for instance feedstock moisture content and reactor diameter and height [11] . Thus, it is clear that experimentation to find optimal conditions to a given gasifier is time consuming and expensive [12]. Mathematical modeling is a convenient alternative to understand the governing principles and optimal points of operation of the gasification process.

There are levels of modeling that, based on their complexity, are capable to represent with more detail the gasification performance. The previous equals to more accuracy in the results expected with the model and better understanding of the key parameters. Zero dimensional modeling is the basic level applied to give a preliminary glimpse of gasification; considered a relation between input and outputs variables but without taking into account the phenomena occurring within the control volume evaluated and the hypothesis of chemical equilibrium ; the changes in the properties along the gasifier are null, this is a disadvantage [9]. On the other hand, dimensional modeling is grounded on chemical kinetics integrated with mass and energy conservation laws. Dimensional models represent

the internal ongoing phenomenon, that is why this kind of modeling allows the study of the four principal stages of gasification [13]. Likewise, dimensional modeling has three categories: One-dimensional models, two-dimensional models and three-dimensional models. In 1D models equilibrium hypotheses are no longer necessary (as well in 2D and 3D models); assume inside variance, only at one space coordinate, of all properties and conditions.1D modeling resembles a plug-flow reactor model [9] .

2D modeling is a tool used when it is necessary to represent variations in a second dimension, for instance, when laminar flow is assumed and the differences in axial and radial directions are important; unlike 1D model where only axial direction changes matters. 3D modeling is the more realistic representation of any process, hence its computational and mathematical complexity. 3D models are practical when, besides radial and axial changes occur, asymmetrical geometries are involved [9]. Dimensional modeling has two considerations; stationary state and transitory state. The first one is assumed when a continuous operation in the gasifier occurs; the process takes long periods of time. Transitory state applies when the gasifier operates for shorts periods of time or during start-ups [14].

Changes in process parameters have a significant effect on the final gas composition and the overall performance, choosing the right level of modeling among the options is essential to guarantee accurate approaches to process parameters. It has to be a down-to-earth decision based on the necessity.

3.3. Background

Numerous studies have modeled gasification processes aiming to simulating under certain conditions the performance of the gasifiers. The classification of the gasification models could be summarized in three types: thermodynamic equilibrium models, kinetic models, CFD (computational fluid dynamics) and ANN (artificial neural network) models [11].

Thermodynamic equilibrium modeling considers a stable system in which the entropy is maximized, while the Gibbs free energy is minimized. These models have reasonable predictions of the final composition and system temperatures; however the assumptions taken in this approach avoid the influence of the design variables within the gasifier [7]. The main limitation of this type of model is their independence of the gasifier design, making them unsuitable to study a specific type of gasifier. Unlike thermodynamic equilibrium models, kinetic models predict the gasifier performance for a given set of operating conditions and specific configurations. Therefore, models represent the reaction networks in the process [11]. Due to its integrated approach of the design variables and reaction kinetics, kinetic models are more accurate than thermodynamic equilibrium models.

CFD models are based on solutions of a set of simultaneous equations for conservation of mass, momentum, energy, and species over a discrete region of the gasifier [7]. CFD

modeling is a highly accuarate model. ANN modeling is a new tendency in gasification modeling. It is limited by the avaliability of databases, however it is expected that as more data becomes available for use in the databases the different reaction networks can be modeled by ANN. [10] Although CFD and ANN are detailed and advanced modeling approaches, they have some limitations. CFD models must have detailed numerical methods for multi-phase flow simulation, which in some cases are difficult to apply [11]. Whereas ANN models cannot produce analytical results but only numerical results, in other words, ANN models work as a “Black Box” which are expected an numerical outcome but have limited ability to identify causal relationships due to their architecture based on in-out nodes. [15]

Besides the different gasification models, there are also different gasifier configurations. In each one of these configurations, the different model types can be applied. The gasifier to be modeled has a downdraft configuration, this means that the fuel and the product gases flow in same direction. Downdraft gasifiers are a kind of fixed-bed gasifiers [7].

Milligan in his PhD thesis [16] developed one of the earliest models of a downdraft gasification of biomass in order to evaluate the reactor length. A thermochemical equilibrium two stages model of the pyrolysis and gasification zone was implemented with the aim of comparing wood char gasification within the gasifier. The pyrolysis zone model had acceptable accuracy; however the length of the gasification zone was not accurate, according to the author, due to the kinetic data used and the pore sized wooden biomass assumed. More recently, several authors have published different downdraft gasification models. Giltrap et. Al [17] formulated a steady state model for the reduction zone based on the kinetic reactions to predict the concentrations of the final products. Zainal et al. [18] modeled a downdraft gasifier for four different biomass materials. The model allowed the prediction of the outlet gas composition and its calorific value. Gøbel et al. [19], developed a mathematical model based on chemical equilibrium. The model was validated experimentally in a 100 kW two-stage gasifier using beech wood chips, and it was able to predict temperature variations and final gas compositions. Melgar and co-workers [20] analyzed a combined model to predict the final composition of the produced gas. The combined model integrated chemical equilibrium and thermodynamic equilibrium. Their objective was to study the influence of the fuel/air ratio on the gasification process. At low fuel/air ratio, high carbon dioxide content was found in the outlet gas.

Besides the development of new models, there are different works in the literature that compare among different types of gasification models. Sharma [21] applying thermodynamic and kinetic modeling compared the gas composition, calorific value and conversion efficiency of both models to experimental data. The kinetic model was found to have better agreement with experimental data.

Janajreh and Shrah [22] developed a numerical simulation using CFD to represent the axial temperatures within a downdraft gasifier. However the average temperatures were not approximate to experimental results; the conclusions reached point out the unfitness of model to emulate the heat losses, basically because it was a small scale gasifier and the average temperatures overcame the experimental ones.

Mathematical gasification models tend to be bulky due to the complexity of the process. Therefore the use of computational tools is common to ease the simulation of the models. There are several different options that have been used to implement and simulate gasification models. FORTRAN is one of the most traditional programming languages used to construct models. Jayah et al. [23] used FORTRAN to simulate a downdraft gasifier for a tea industry. Some authors have simulated gasification model by using MS Excel with VBA (Visual Basic Applications). Its familiar interface and ease of use are some of the main advantages considered when using this approach. However, the processing capabilities of the program are limited compared to other options. Budhathoki in his master thesis [7] implemented a three zone model of downdraft gasification in MS Excel. Moreover, MATLAB is a computing software commonly used to simulate models. Its massive computing capabilities and wide academic adoption have made it in one of the most common tools for simulation of different models. Pérez et al. [24] programmed a fixed bed downdraft biomass gasification model in MATLAB. Others researchers have opted for simpler ways to represent gasification models. Aspen Plus is a problem-oriented software that integrates physical, chemical and biological principles into its computing structure was used by Arnavat et al. [25]. Although the latter alternative simplifies modeling, the rigid structure of predefined model structures of software like Aspen Plus limits the applicability of this approach.

The gasification modeling prospect is encouraging, range of approaches in gasification models allow evaluation of elaborate heat losses system, set up of physical specs and even process refining for select components in final syngas. Studies addressed above show a wide and diverse field which, depending on the reach desired, is feasible analyze gasification as merely transformation process and as practical method for energy generation in which fine tuning and optimal operation of equipment are achievable via modeling.

Chemical kinetic modeling is an appropriate approach to address the objectives. The capability to predict compositions of the produced gas is inherent into this kind of modeling. Besides, kinetic modeling allows the understanding of biomass transformation due to its integrated chemistry of the reactions involved in the process with the design variables of the gasifier; stage by stage analysis would be possible. It is worth noting that because of its accuracy this kind of modeling is computationally intensive. Therefore, as an initial approach to the problem of modeling a downdraft gasifier kinetic models will be used as the base for this project. This model was programmed in MATLAB, which is convenient software for the simulation of different processes and includes a large library of mathematical operations that would allow an adequate implementation of the model of the gasifier.

4. Considerations and assumptions

Model considerations

- Level of modelling: One-dimensional modeling is a suitable level for the objectives of this work. Axial evaluations of the process along the length of the gasifier allows an integral analysis of biomass gasification, and with the hypothesis taken in this level of modeling the results, according to the literature, are approximate to experimental ones.

- State: steady state, this is an assumption that can be made because most fixed bed gasifiers operate for long periods of time [9]. . Likewise isobaric state (at atmospheric pressure operation).

- Type of model: a chemical kinetic model allows dividing the process into stages, in order to evaluate each one individually with their respective chemistry.

- Gasification stages: The model will preserve the four essentials gasification stages: drying, pyrolysis, oxidation and reduction. Although some studies include coupled stages, the present work separates each of the stages and their interaction.

- Tars definition: Thuman et al. defined tars as a gas mixture of primary and secondary hydrocarbons with general chemical formula $C_6H_{6.2}O_{0.2}$. The model takes that assumption considering the high temperatures of the process, which prevent tars' condensation [26].

- Ashes are considered an inert element.

- Gas phase behavior: The expected conditions of the process (temperature and pressure) and the substances involved can be represented by ideal gas. This condition applies for the gas species and the resulting product: syngas
- Mass aspects: mass conservation subject to chemical kinetics rates and stoichiometric coefficients of the chemistry of each stage. Mass transfer through is not considered due to its small effect compared to convective mass transfer, which is more relevant [13].

- Energy aspects: Adiabatic assumption in the system gasifier-surroundings and interactions only between solid and gas phases – convective heat transfer-, as well as energy associated with the chemical kinetics.

5. Model description

The model described below comprises the processes of drying, pyrolysis, oxidation and reduction. Those processes involve mass and energy transfer phenomena, as well as homogenous and heterogonous reactions. The dimensional model divides the gasifier into two phases: solid and gas. It is proposed as an initial-value problem for the solution of the system of differential algebraic equations (DAE), where biomass flow and the equivalence ratio are the initial values. The model considers two different phases: solid and gas. Each phase contains different species, and has a different mathematical treatment in the model. Tables 1 and 2 list the species in the gas and solid phases of the model, respectively.

Table 1. Gas phase species

Species	Symbol
Carbon dioxide	CO_2
Carbon monoxide	CO
Hydrogen	H_2
Oxygen	O_2
Nitrogen	N_2
Methane	CH_4
Tars	tars
Water vapor	H_2OV

Table 2. Solid phase species

Species	Symbol
Moisture	H_2OL
Biomass	bms
Char	char

5.1 Biomass treatment

Biomass, as fuel of the gasification process, has to be characterized with different analyses, which will be used as input to the model. It is required to know the biomass' composition and properties to allow the model to simulate the process.

- *Elemental analysis* defines carbon (C), hydrogen (H), nitrogen (N), sulfur (S) and oxygen (O) mass fractions within biomass.
- *Proximate analysis* establishes carbon fixed (%CF), moisture (moi), ash and volatile mass percentage of the biomass.
- *Specific density* -deducting pore volume-(ρ_{bms}) *and calorific value*

With the information provided by the analyses is possible to define: molecular weight of biomass (W_{bms}), initial biomass flow (n_{bms}), initial moisture flow (n_{moi}) and initial char flow (n_{char}).

- Biomass molecular weight

Mass fractions of the elemental analysis enable calculate coefficients of biomass chemical formula $C_nH_mO_p$, using as reference 1 atom of carbon n=1 and with the molecular weight (W_i).

$$m = \frac{H \cdot Wc}{C \cdot W_H} \;\; ; \;\; p = \frac{O \cdot Wc}{C \cdot Wo} \;\; ; \;\; q = \frac{N \cdot Wc}{C \cdot W_N} \;\; ; \;\; r = \frac{S \cdot Wc}{C \cdot Ws} \qquad [E.1]$$

However, due to the low contents of nitrogen and sulfur in common biomass products, the model only considers carbon, oxygen and hydrogen for the kinetics. Although for the equivalent ratio of gasifying agent all elements present in the biomass are considered [13].

Once the biomass molecular weight is known, the relative humidity is converted into molar fraction of moisture in biomass (*w*).

$$w = \frac{W_{bms} \cdot moi}{W_{H2o} \cdot (1 - moi)} \qquad [E.2]$$

Initial molar concentration of carbon within biomass is define by

$$C_{char,bms} = 1{,}000 \cdot \%CF \cdot \frac{\rho_{bms}}{w_{char}} \qquad [E.3]$$

- Equivalence ratio (ER)

Air to fuel Equivalence ratio (ER) indicates the relation between the ratio of gasifying agent flow and fuel (m_{bms}), and the ratio of stoichiometric gasifying agent flow to fuel ($ER_{stoichiometric}$.) As mentioned before, gasifying agent flow is an operational parameter; however the equivalence ratio is commonly used to define it [7].

$$ER_{operational} = \frac{m_{bms}}{m_{g.a}} \quad [E.4]$$

$ER_{stoichiometric}$ is constant for a specific biomass and depends on the Elemental analysis.

$$ER_{stoichiometric} = \left(1 + \frac{m}{4} - \frac{p}{2}\right) \cdot \left(\frac{W_{O_2} + 3.76 \cdot W_{N_2}}{W_{bms}}\right) \quad [E.5]$$

Finally the real gasifying agent flow is defined, knowing ER, $ER_{stoichiometric}$ and the biomass flow(m_{bms}):

$$ER = \frac{ER_{operational}}{ER_{stoichiometric}} = \frac{m_{bms}/m_{g.a}}{ER_{stoichiometric}} \quad [E.6]$$

5.2 Drying model

The moisture passes from a liquid to a vapor state. The kinetic constant is Arrhenius type (see Table 3). The sub model is adapted from Bryden et al. [27], However the condensation of the vapor is not taken into account.

$$H_2OL \xrightarrow{k_d} H_2OV \qquad [R.1]$$

Table 3. Kinetic constants and reaction rates of drying

$\tilde{r}_j$	k_j	A_j [s^{-1}]	E_j [kJ/mol]
$\tilde{r}_d = k_d C_{H2OL}$	k_d	5.13e10	88.0

In the drying sub model is defined the consumption of the biomass' moisture that is converted in vapor. The importance lies in that the energy needed to evaporate the moisture affects greatly the others processes, this is one of the reasons to opt for preheating processes of the biomass.

5.3 Pyrolysis model

The work proposed by Bryden et al. [27] is chosen to represent the sub process of pyrolysis. The model represents the thermal chemical transformation into three parallel reactions; Table 4 contains the kinetic constants:

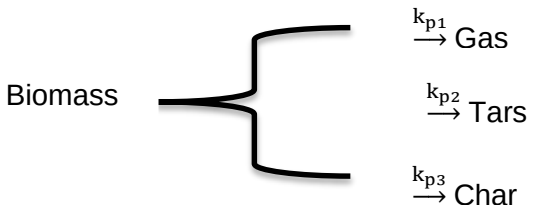

[R.2]

In order to disaggregate the composition of the gas the model of composition pyrolysis sub model of Thuman et al. [26] is used. The volatile species integrated are: CO_2, CO, H_2OV, CH_4, H_2 and tars. The sub model consists of a system of six equations described below and three mass ratios ($\Omega_1, \Omega_2, \Omega_3$). In this part of the model the temperature is assumed to be 800 K (average pyrolysis temperature for wooden biomass):

$$C_nH_mO_p \longrightarrow \nu_{H_2OV,p} + \nu_{H_2,p} + \nu_{CO_2,p} + \nu_{CO,p} + \nu_{CH_4,p} + \nu_{tars,p} + Y_{char} \quad [R.3]$$

$$\Omega_1 = 1.94 \cdot 10^{-6} \cdot T^{1.87} \quad [E.7]$$

$$\Omega_2 = 1.305 \cdot 10^{-11} \cdot T^{3.39} \quad [E.8]$$

$$\Omega_3 = 0.85 - 0.95 \quad [E.9]$$

The system of equations is constituted by three equations representing an atomic balance of species and three empiric correlations.

$$n = \nu_{CO_2,p} + \nu_{CO,p} + \nu_{CH_4,p} + 6 \cdot \nu_{tars,p} + Y_{char} \quad [E.10]$$

$$m = 2 \cdot \nu_{H_2OV,p} + 2 \cdot \nu_{H_2,p} + 4 \cdot \nu_{CH_4,p} + 6{,}2 \cdot \nu_{tars,p} \quad [E.11]$$

$$p = \nu_{H_2OV,p} + 2 \cdot \nu_{CO_2,p} + 4 \cdot \nu_{CO,p} + 0{,}2 \cdot \nu_{tars,p} \quad [E.12]$$

$$\frac{\nu_{CO,p}}{\nu_{CO_2,p}} = \Omega_1 \cdot \frac{w_{CO_2}}{w_{CO}} \quad [E.13]$$

$$\frac{\nu_{CH_4,p}}{\nu_{CO_2,p}} = \Omega_2 \cdot \frac{w_{CO_2}}{w_{CH_4}} \quad [E.14]$$

$$\frac{\nu_{H_2OV,p}}{\nu_{CO_2,p}} = \Omega_2 \cdot \frac{w_{CO_2}}{w_{H_2OV}} \quad [E.15]$$

Table 4. Kinetic constants and reaction rates of pyrolysis

$\tilde{r}_j$	k_j	A_j [s^{-1}]	E_j [kJ/mol]
$\tilde{r}_{p1} = k_{p1} C_{bms}$	k_{p1}	1.44e4	88.6
$\tilde{r}_{p2} = k_{p2} C_{bms}$	k_{p2}	4.13e6	112.7
$\tilde{r}_{p3} = k_{p3} C_{bms}$	k_{p3}	7.38e5	106.5

In this model is established the rates of production of each specie, starting from an empirical sub model, which uses the stoichiometric coefficients of each volatile specie ($\nu_{i,p}$) produced by the pyrolyzed biomass.

5.4 Oxidation model

This sub model consists of homogeneous and heterogeneous reactions, the volatile gases and char formed previously by pyrolysis, are oxidized with the incoming gasifying agent. Pérez [13], summarized the phenomena with the following chemical mechanism and their respective kinetic constant are in Table 5:

$$C_6H_{6.2}O_{0.2} + 2.9\ O_2 \xrightarrow{k_{c1}} 6\ CO + 3.1\ H_2 \quad [R.4]$$

$$CH_4 + 1.5\ O_2 \xrightarrow{k_{c2}} CO + 2\ H_2O \quad [R.5]$$

$$2\ CO + O_2 \xrightarrow{k_{c3}} 2\ CO_2 \quad [R.6]$$

$$2\ H_2 + O_2 \xrightarrow{k_{c4}} 2\ H_2O \quad [R.7]$$

$$2C + O_2 \xrightarrow{k_{c5}} 2\ CO \quad [R.8]$$

Table 5. Kinetic constants and reaction rates of oxidation

$\tilde{r}_j$	k_j	A_j	A_j Units	E_j [kJ/mol]
$\tilde{r}_{c1} = k_{c1} T_g P^{0.3} C_{tars}^{1/2} C_{O2}$	k_{c1}	59.8	$kmol^{-0.5} m^{1.5} K^{-1} Pa^{-0.3} s^{-1}$	101.43
$\tilde{r}_{c2} = k_{c2} T_g C_{CH4}^{1/2} C_{O2}$	k_{c2}	9.2e6	$(m^3 mol^{-1})^{-0.5} (K\ s)^{-1}$	80.23
$\tilde{r}_{c3} = k_{c3}\ C_{CO}\ C_{O2}^{1/4} C_{H2OV}^{1/2}$	k_{c3}	$10^{17.6}$	$(m^3 mol^{-1})^{-0.75} s^{-1}$	166.28
$\tilde{r}_{c4} = k_{c4}\ C_{H2}\ C_{CO2}$	k_{c4}	1e11	$m^3 mol^{-1} s^{-1}$	42.00
$\tilde{r}_{c5} = 2 \left(\frac{w_{char}}{w_{O2}}\right) v_p \left(\frac{k_{c5}\ h_{m,c5}}{k_{c5} + h_{m,c5}}\right) C_{O2}$	k_{c5}	1.7 T_s	ms^{-1}	74.83

5.5 Reduction model

The sub model of reduction embraces the reduction zone study of Giltrap et al. [17] Three heterogeneous reactions of char and gas species are considered. An additional homogenous reaction known as *steam reforming of methane* is also considered.

$$C + CO_2 \xrightarrow{k_{g1}} 2\,CO \qquad [R.9]$$

$$C + 2H_2 \xrightarrow{k_{g2}} CH_4 \qquad [R.10]$$

$$C + H_2O \xrightarrow{k_{g3}} CO + H_2 \qquad [R.11]$$

$$CH_4 + H_2O \xrightarrow{k_{g4}} CO + 3\,H_2 \qquad [R.12]$$

Pérez [13] suggest others common chemical reactions that take place in gasification processes one commonly known as water *gas shift reaction*:

$$C_6H_{6.2}O_{0.2} + 5.8H_2O \xrightarrow{k_{g5}} \mathbf{6}CO + 8.9\,H_2 \qquad [R.13]$$

$$CO + H_2O \xleftrightarrow{k_{wg}} CO_2 + H_2 \qquad [R.14]$$

Table 6 summarizes the kinetic constants for the reduction zone and the formula for the heterogeneous reaction rates. Section 5.7 explain the procedure to calculate the diffusion coefficients ($h_{m,i}$) .

Table 6. Kinetic constants and reaction rates of reduction

$\tilde{r}_j$	k_j	A_j	A_j Units	E_j [kJ/mol]
$\tilde{r}_{g1}=\left(\frac{w_{char}}{w_{CO2}}\right) v_p \left(\frac{k_{g1}\, h_{m,g1}}{k_{g1}+ h_{m,g1}}\right) C_{CO2}$	k_{g1}	3.42 T_s	ms^{-1}	129.7
$\tilde{r}_{g2}=0.5 \left(\frac{w_{char}}{w_{H2}}\right) v_p \left(\frac{k_{g2}\, h_{m,g2}}{k_{g2}+ h_{m,g2}}\right) C_{H2}$	k_{g2}	1e-3 k_{g1}	ms^{-1}	129.7
$\tilde{r}_{g3}=\left(\frac{w_{char}}{w_{H2OV}}\right) v_p \left(\frac{k_{g3}\, h_{m,g3}}{k_{g3}+ h_{m,g3}}\right) C_{H2OV}$	k_{g3}	1.67 k_{g1}	ms^{-1}	129.7
$\tilde{r}_{g4}= k_{g4}\, C_{H2OV} C_{CH4}$	k_{g4}	3015	$m^3mol^{-1}s^{-1}$	125.52
$\tilde{r}_{g5}= k_{g5}\, C_{tars}^{0.25} C_{H2ov}^{1.25}$	k_{g5}	70	$m^3mol^{-1}s^{-1}$	16.736
$\tilde{r}_{wg}=k_{wg}\left(C_{CO} C_{H2ov} - C_{CO2} C_{H2}/K_{wge}\right)$	k_{wg}	2.78	$m^3mol^{-1}s^{-1}$	32.9
	k_{wge}	0.0265	--	--

5.6 Solid-Gas heat transfer

Heat transfer between solid and gas phases is modeled after the work of Di Blasi [28] for non-reacting systems with an empirical factor of correction ζ (0.02-1) which balance the deviation between of theoretical and experimental values.

The energy transfer between the solid and the gas is given by:

$$Q_{sg} = \zeta \cdot h_{sg} \cdot v_p \cdot \left(T_s - T_g \right) \qquad [E.16]$$

Where the solid/gas heat transfer coefficient is:

$$h_{sg} = \frac{Nu \cdot k_g}{d_p} \qquad [E.17]$$

Perez [13], reviews the specific expressions, for packed beds, of the next adimensional correlations:

$$Nu = 2 + 1.1 \cdot Re^{0.6} \cdot Pr^{\frac{1}{3}} \qquad [E.18]$$

$$Pr = \frac{C_{p,g}}{\mu_g \cdot k_g} \qquad [E.19]$$

$$Re = \frac{\rho_g \cdot d_p \cdot u_g}{\mu_g} \qquad [E.20]$$

5.7 Heterogeneous and homogeneous reactions

Mass and energy conservation laws require rates of production or consumption of each specie. Gasification process comprehends gas-gas reactions (homogenous) and solid-gas reactions (heterogeneous).

The net production or consumption rates of species are determined as follows:

$$\widetilde{\mathrm{r_i}} = \sum_{\mathrm{j}} \nu_{\mathrm{i,j}} \cdot \widetilde{\mathrm{r_i}} \qquad [\mathrm{E.21}]$$

$$\mathrm{j} = \text{chemical reaction};\ \mathrm{i} = \text{specie}$$

Based on the kinetics of each sub model, stoichiometric coefficients $\nu_{i,j}$ and the rate of reaction $\widetilde{r_i}$, the net rates of each species are calculated. The rate of reaction depends on the reaction temperature and the concentration of the species. Furthermore, depending on the consumption or appearance of the species, the stoichiometric coefficients $\nu_{i,j}$ are either positive or negative.

All the sub models have Arrhenius type kinetics for the kinetic constants. However, homogenous and heterogeneous reactions differ in how the mass transfer coefficients are determined. Heterogeneous rate constants might be limited by mass transfer, whereas homogeneous reactions are not largely affected by diffusion.

The expression below describes the mass transfer coefficient for homogenous reactions:

$$\mathrm{k_j} = \mathrm{A_j} \cdot \exp \cdot \left(\frac{-\mathrm{E_j}}{\mathrm{R} \cdot \mathrm{T}}\right) \qquad [\mathrm{E.22}]$$

For heterogeneous reactions in oxidation and reduction zones is necessary to use an effective reaction rate ($\boldsymbol{k_e}$) due to diffusion interactions between the solid (char) and the gas species:

$$k_e = \frac{\mathrm{k_c} \cdot \mathrm{h_{m,j}}}{\mathrm{k_c} + \mathrm{h_{m,j}}} \qquad [\mathrm{E.23}]$$

Where the mass diffusion coefficient ($h_{m,i}$) is given by:

$$h_{m,i} = \frac{Sh \cdot D_j}{d_p} \qquad [E.24]$$

$$i = c5, g1, g2, g3 \; ; j = O_2, CO_2, H_2, H_2O$$

The diffusion coefficients (D_j) are listed in Table 7.

The adimensional Sherwood and Schmidt numbers can be determined from the following correlations::

$$Sh = 0.9 \left(2 + 0.6 \cdot Re^{0.6} \, Sc^{\frac{1}{3}} \right) \qquad [E.25]$$

$$Sc = \frac{\mu_g}{\rho_g \cdot D_j} \qquad [E.26]$$

Table 7. Diffusion coefficients for heterogeneous reactions

Reaction/Notation	Diffusion coefficient [$m^2 s^{-1}$]
$\tilde{r}_{c5}/D_{O2}$	7.22e-4
$\tilde{r}_{g1}/D_{CO2}$	6.16e-4
$\tilde{r}_{g2}/D_{H2}$	28.89e-4
$\tilde{r}_{g3}/D_{H2O}$	9.63e-4

The parameters for the kinetics constant of each reaction are summarized in the corresponding sub model section.

5.8 Dimensional and geometric parameters

This section describes the parameters linked to the gasifier geometry and its relation with the biomass specifications. The areas and volume are subject to changes in the axial axis ΔZ, the void fraction, solid and gas areas and the density number of particle are fixed for the entire simulation.

- **Void fraction:** Space filled by gas phase within the gasifier [13]**.**

$$\epsilon = 0.38 + 0.073 \cdot \left(1 + \frac{\left(\frac{d_t}{d_p} - 2\right)^2}{\left(\frac{d_t}{d_p}\right)^2} \right) \quad [E.27]$$

- **Area and volume:** subject of the geometric of the gasifier and assuming a constant cylindrical form of gasifier.

$$A = \pi \cdot \left(\frac{d_t}{2}\right)^2 \quad [E.28]$$

$$V = \pi \cdot \left(\frac{d_t}{2}\right)^2 \cdot h \quad [E.29]$$

- **Solid and gas areas:** With the void fraction is possible to determine the relation between the total volume and the volume occupied of the gas and solid phases.

$$A_g = \epsilon \cdot A \quad [E.30]$$

$$A_s = (1 - \epsilon) \cdot A \quad [E.31]$$

- **Density number of particle:**

$$v_p = \frac{6 \cdot (1 - \epsilon)}{d_p} \quad [E.32]$$

5.9 Continuity Equations

The derivation of continuity equations is based on several works [9,13,27,28] that deepen into the mathematical demonstration. As discussed in section 3.2, unidimensional modeling does not consider angular and radial effects, based on cylindrical coordinates, and only considers axial effects. Equations are based on a volume differential (ΔV) of diameter d_t and thickness ΔZ.

Mass conservation:

The model is considered in steady state. Therefore, accumulation of species in the system is neglected. Likewise mass rate by diffusion is not considered due to its slight effect. Starting from the aforementioned considerations, for i (species):

$$\text{accumulative net rate of i} = \text{convective net rate of i} + \text{diffusion net rate of i}$$

$$+ \text{chemical reaction production net rate of i}$$

Where the net rate of species entering and exiting in the volume differential is (ΔV):

$$\frac{d}{dz}(A_j(z) \cdot C_i \cdot u_j) \qquad [E.33]$$

Abbreviating

$$n_i = A_j(z) \cdot C_i \cdot u_j \qquad [E.34]$$

The net rate of production by chemical reaction is:

$$\sum \tilde{r}_i \cdot A_j(z) \qquad [E.35]$$

Finally, the molar flow within a volume differential (ΔV)

$$\frac{dn_i}{dz} = \sum \tilde{r}_i \cdot A_j(z) \qquad [E.36]$$

With these considerations the complete set of balance equations for all the components can be derived. Below are described each of these equations, arranged by phase.

Solid phase

$$\frac{dn_{bms}}{dz} = -A_s \cdot \tilde{r}_p \quad [E.37]$$

$$\frac{dn_{H_2OL}}{dz} = -A_s \cdot \tilde{r}_d \quad [E.38]$$

$$\frac{dn_{char}}{dz} = A_s \cdot \sum_j \nu_{char,j} \cdot \tilde{r}_j \quad [E.39]$$

Gas phase

$$\frac{dn_{CO}}{dz} = \sum_j A_i \cdot \nu_{CO,j} \cdot \tilde{r}_j \quad [E.40]$$

$$\frac{dn_{CO_2}}{dz} = \sum_j A_i \cdot \nu_{CO_2,j} \cdot \tilde{r}_j \quad [E.41]$$

$$\frac{dn_{H_2}}{dz} = \sum_j A_i \cdot \nu_{H_2,j} \cdot \tilde{r}_j \quad [E.42]$$

$$\frac{dn_{CH_4}}{dz} = \sum_j A_i \cdot \nu_{CH_4,j} \cdot \tilde{r}_j \quad [E.43]$$

$$\frac{dn_{tars}}{dz} = \sum_j A_i \cdot \nu_{tars,j} \cdot \tilde{r}_j \quad [E.44]$$

$$\frac{dn_{H_2OV}}{dz} = \sum_j A_i \cdot \nu_{H_2OV,j} \cdot \tilde{r}_j \quad [E.45]$$

$$\frac{dn_{O_2}}{dz} = \sum_j A_i \cdot \nu_{O_2,j} \cdot \tilde{r}_j + \nabla_{O_{2,ag}} \quad [E.46]$$

$$\frac{dn_{N_2}}{dz} = \nabla_{N_{2,ag}} \quad [E.47]$$

$$j = d, \tilde{p}, c1, c2, c3, c4, c5, g1, g2, g3, g$$

Energy conservation

The energy balance is set to a volume differential in the gasifier for both phases. Accumulative energy rate, radiation effects and energy exchange between wall and surroundings are not considered. Moreover, thermal conductivity is not included either.

The energy balance across transversal section becomes:

$$\text{energy rate entering and exiting} = \text{solid/gas energy exchange rate}$$

$$+\text{energy rate associated to chemical species}$$

In Di Blasi [28] the energy source term associated to the chemical reactions is treated as a path function, hence the heat of the reaction is calculated applying Hess' Law. Although, initially Di Blasi present energy conservation equations with second derivatives (thermal conductivity term), Seggiani [29] adapts it to first order differential obviating thermal conductivity, phenomena out of the model scope.

$$dH_s = A_s \cdot C_s \cdot h_{T,i} \cdot u_s \qquad [E.48]$$

$$\frac{dH_s}{dz} = -A_s \cdot Q_{sg} + (-\Delta H)_{dry} \cdot \tilde{r_d} + \sum_j (-\Delta H_i) * \tilde{r}i \qquad [E.49]$$

$$j = bms, char, moi; \quad i = d, c5, g1, g2, g3$$

$$dH_g = A_g \cdot C_g \cdot h_{T,i} \cdot u_g \qquad [E.50]$$

$$\frac{dH_g}{dz} = -A_s \cdot Q_{sg} - \sum_j (-\Delta H_i) * \tilde{r}i \qquad [E.51]$$

$$j = H_2OV,\ H_2, CO, CO_2, CH_4, tars; i = c1, c2, c3, c4, g4, g5$$

- **Solid and gas temperatures**

The differential equations of the model are in terms of energy flow, thus it is necessary know the temperature of each phase because the kinetic constants depend on the temperatures to be calculated.

Heat transfer in each phase has the following form [13]:

$$H_j = \sum_j n_i \cdot \left(h°_{f,i} + \int_{Tref}^{T_j} Cp_i \cdot dT \right) \qquad [E.54]$$

$$j = \text{gas or solid}; i = \begin{cases} \text{if } j = \text{solid};\ \text{bms}, \text{moisture}, \text{char} \\ \text{if } j = \text{gas}; O_2, N_2, H_2OV, H_2, CO, CO_2, CH_4, \text{tars} \end{cases}$$

From the energetic equation above, the equation to define the temperature of each phase can be obtained as:

$$T_{k+1} = T_k + \frac{H_j + \sum_j n_i \cdot (h°_{f,i} + \int_{Tref}^{T_j} Cp_i \cdot dT)}{\sum_j Cp_i(T_k)} \qquad [E.55]$$

$$i = \begin{cases} \text{if } j = \text{solid};\ \text{bms}, \text{moisture}, \text{char} \\ \text{if } j = \text{gas};\ O_2, N_2, H_2OV, H_2, CO, CO_2, CH_4, \text{tars} \end{cases}$$

The temperature for the next axial position (T_{k+1}) is estimated from the previous temperature T_k and the properties calculated in step k. The numerical method implemented advances gradually the length Z (for a detailed explanation see section 6.1). Table 12 and 13 summarizes the correlations employed for solid and gas species, respectively.

6. Algorithm development

The model was programmed in MATLAB R2010a. The differential algebraic system (DAE) is composed of integrated variables (molar flow of species and energy flow of phases) and non-integrated variables (solid and gas volumes, kinetics rates and temperatures), which are solved for the total volume of the gasifier (V). Originally fourth-order Runge-Kutta was used to solve the system. However, due to the stiffness of the model MATLAB subroutine ODE15s was implemented instead. Figure 2 depicts the step-by-step procedure of the algorithm.

Besides solving simultaneously the four stages of the gasifier (see Fig. 1) the model was divided into two segments, drying and pyrolysis process were solved first and their results were used as inputs to the second oxidation and reduction process.

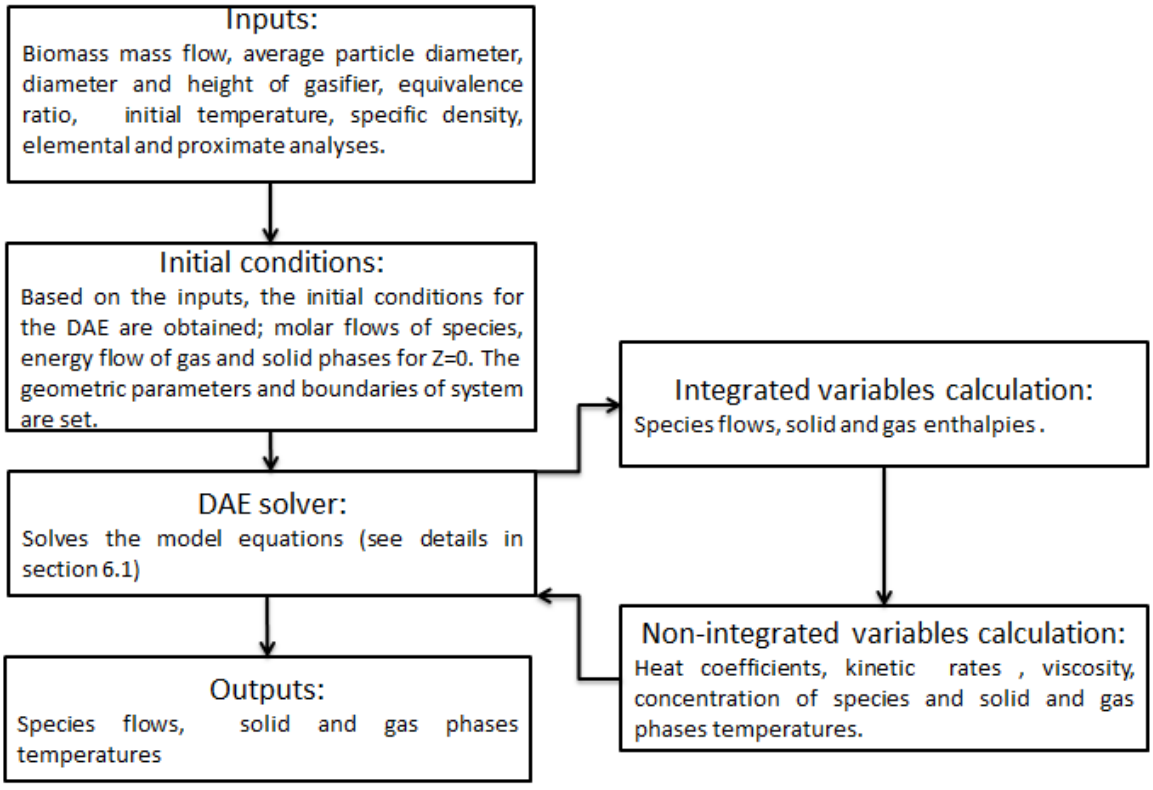

Figure 2. Block diagram of the gasifier model implemented in Matlab.

6.1 Numerical method to solve DAE

MATLAB incorporates a set of standard routines in form of functions to solve DAE. In this work, the model is solved using ODE15s function. Initially fourth-order Runge-Kutta (RK4) was integrated to the code developed. However, the stiffness of the model did not allow for a successful implementation and the pre-built Matblab function ODE15s was used instead. The latter is an implementation of implicit Runge-Kutta method. Details of the methods to solve DAE are presented next:

- **Fourth-order Runge-Kutta (RK4)**

RK4 is one of the most widely used numerical integration method for ordinary differential equations [30]. And RK4 allows the progressive evaluation of the different points of the total length. Besides, using RK4 help to a better understanding of the system solution and as an academic enforcement of tools learned.

Following is the solution method for the differential equations is described. First, as a simplification of the notation, the following consideration is taken:

$$\frac{dx_1}{dy} = x'_1 \qquad [E.56]$$

A system of N equations assorted like

$$x'_1 = f(t, x_1, x_2, \dots, x_N) \qquad [E.57]$$

$$x'_2 = g(t, x_1, x_2, \dots, x_N) \qquad [E.58]$$

$$\dots$$

$$x'_N = q(t, x_1, x_2, \dots, x_N) \qquad [E.59]$$

With the known initial values of each equation.

.

$$x_1(t_0) = x_{1,0} \qquad [E.60]$$

$$x_2(t_0) = x_{2,0} \qquad [E.61]$$

$$\dots$$

$$x_N(t_0) = x_{N,0} \quad [E.62]$$

This system of equations can be solved by RK4. The solution in a point is evaluated using the previously calculated value. The expressions to determine the derivatives are:

:

$$x'_{1,n+1} = x'_{1,n} + \frac{h}{6}(F_1 + 2F_2 + 2F_3 + F_4) \quad [E.63]$$

$$x'_{2,n+1} = x'_{2,n} + \frac{h}{6}(G_1 + 2G_2 + 2G_3 + G_4) \quad [E.64]$$

…

$$x'_{N,n+1} = x'_{N,n} + \frac{h}{6}(Q_1 + 2Q_2 + 2Q_3 + Q_4) \quad [E.65]$$

Where h is the interval of the independent variable, in the case of the gasifier model developed h is defined as ΔZ. Runge Kutta factors (F, G, …., Q) are defined below

$$F_1 = f(t_n, x_{1,n}, x_{2,n}, \dots., x_N) \quad [E.66]$$

$$F_2 = f\left(t_n + \frac{1}{2}h, x_{1,n} + \frac{1}{2}h \cdot F_1, x_{2,n} + \frac{1}{2}h \cdot G_1, \dots., x_{N,n} + \frac{1}{2}h \cdot Q_1\right) \quad [E.66]$$

$$F_3 = f\left(t_n + \frac{1}{2}h, x_{1,n} + \frac{1}{2}h \cdot F_2, x_{2,n} + \frac{1}{2}h \cdot G_2, \dots., x_{N,n} + \frac{1}{2}h \cdot Q_2\right) \quad [E.67]$$

$$F_4 = f(t_n + h, x_{1,n} + h \cdot F_3, x_{2,n} + h \cdot G_3, \dots., x_{N,n} + h \cdot Q_3) \quad [E.68]$$

$$G_1 = g(t_n, x_{1,n}, x_{2,n}, \dots., x_N) \quad [E.69]$$

$$G_2 = g\left(t_n + \frac{1}{2}h, x_{1,n} + \frac{1}{2}h \cdot F_1, x_{2,n} + \frac{1}{2}h \cdot G_1, \dots., x_{N,n} + \frac{1}{2}h \cdot Q_1\right) \quad [E.70]$$

$$G_3 = g\left(t_n + \frac{1}{2}h, x_{1,n} + \frac{1}{2}h \cdot F_1, x_{2,n} + \frac{1}{2}h \cdot G_1, \dots., x_{N,n} + \frac{1}{2}h \cdot Q_1\right) \quad [E.71]$$

$$G_4 = g(t_n + h, x_{1,n} + h \cdot F_3, x_{2,n} + h \cdot G_3, \dots., x_{N,n} + h \cdot Q_3) \quad [E.72]$$

…

$$Q_1 = q(t_n, x_{1,n}, x_{2,n}, \dots., x_N) \quad [E.73]$$

$$Q_2 = q\left(t_n + \frac{1}{2}h, x_{1,n} + \frac{1}{2}h \cdot F_1, x_{2,n} + \frac{1}{2}h \cdot G_1, \ldots., x_{N,n} + \frac{1}{2}h \cdot Q_1\right) \quad [E.74]$$

$$Q_3 = q\left(t_n + \frac{1}{2}h, x_{1,n} + \frac{1}{2}h \cdot F_1, x_{2,n} + \frac{1}{2}h \cdot G_1, \ldots., x_{N,n} + \frac{1}{2}h \cdot Q_1\right) \quad [E.75]$$

$$Q_4 = q\left(t_n + h, x_{1,n} + h \cdot F_3, x_{2,n} + h \cdot G_3, \ldots., x_{N,n} + h \cdot Q_3\right) \quad [E.75]$$

Unfortunately, when the debugging process was carried out, RK4 did allow for a stable solution to the DAE system. The stiffness of the system made the numerical method slow and inconvenient. Moreover, the iteration process for the integrated variables calculation (see Fig. 2). This was caused by large oscilations in the solution of the DAE with small changes in the initial values. This scenario is problematic for a key variable in the model such as temperature, which affects most of the continuity equations of the model. The RK4 implementation is included in the Appendix as a reference only, and was not used for the results presented in this report.

- **ODE15s**

Although initially the system of equations was implemented using the RK4 procedure, it was not possible to solve the system without using more robust subroutines. Hence, the standard routines included in Matlab for the solution of differential equations were used instead. ODE15s subset routine was implemented due to its suitable performance for one dimensional problems and kinetic systems [31]. DAE systems tend to be stiff or rigid, meaning that some solutions of the equations vary slowly while others vary rapidly. Therefore, the numerical method used to solve them cannot use the same length in each step of the subroutine [32].

ODE15s is intended to solve stiff systems with algebraic expressions. Then it is useful, to calculate the iterative process for the temperature with its inner numerical method.

Execution of the subroutine for the gasifier model requires as input: the length of gasifier (zspan), the initial conditions of the differential equations at length zero (z0), the kinetic constants and the functions for the differential equations. The implementation of ODE15s for the gasifier model used in this work is presented in the Appendix.

6.2 Algorithm structure

The algorithm structure is essential to improving the execution of codes. Firstly, the model proposed was structured in a linear and basic logic. After some attempts, the results of the model showed up and it was not clear to identify possible mistakes. The code was messy and not easy to follow. What some call “Spaghetti code”. Therefore the model was restructured into a more readable programing, taken on the premise that the chosen model, with its assumptions and constrains, could carry through an approximated simulation of a downdraft gasifier. The restructured code has a matrix structure, more efficient. The validation was performed through this code.

In Appendix is presented both programming structures of the model.

7. Validation

Model validation with experimental data is essential to verify the accuracy of the model developed. Jayah et al. [23] results have been used previously to validate simulation models ([13], [7], [33]). The input parameters for this work are shown in Table 8. The experimental analysis for the resulting gas was performed using gas liquid chromatography for CO_2, H_2, CO, CH_4, and N_2. The biomass used was rubber wood. In Tables 9 and 10 are included its ultimate and proximate analyses, respectively. These paremeters were used as parameters of the model and used to calculate the boundary conditions (see Fig. 1).

Table 8. Experimental parameters **[23]** used as input for the model developed.

Parameters	**Value**
Gasifier design	Downdraft gasifier
Fuel	Rubber wood
Fuel density (kg/m^3)	320
Fuel size (cm)	4.4
Diameter (m)	0.92
Gasification zone length (m)	0.220
Length (m)	1.15
Thermocouples	12 type K & T
Gas analyzer	Gas liquid chromatography Carboxen 1000 column

Table 9. Proximate analysis of rubber wood **[23]**.

Property	**Proximate (%d.b.)dry basis**
Volatile matter	80.1
Fixed carbon	19.2

Ash content	0.7

Table 10. Biomass ultimate analysis of rubber wood **[23]**

Biomass material	(%) Rubber wood
C	50.6
H	6.5
N	0.2
O	42
Ash	0.7

As aforementioned the simulations of the gasification model were performed in two different ways: (i) integrating all four stages in one run and (ii) completing a two segments calculation. The results of each of the simulation runs are presented in the following sections.

- **Complete four-stages simulations**

Figure 3, shows the predictions of the developed model for the molar flow of the species throughout the gasifier, for the solid and gas phases respectively.

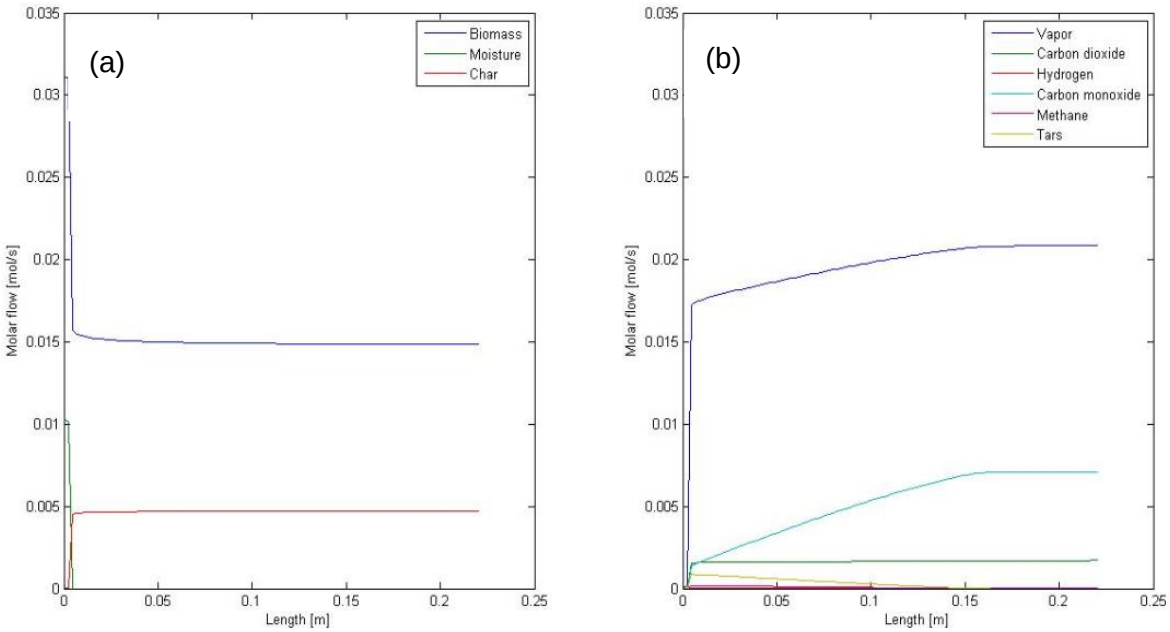

Figure 3. Axial profile of solid phase (a) and gas phase (b) species flows for complete gasification

The behavior represented in figure 3, shows an incomplete gasification. Biomass' drying is reached almost instantly, seen from the sharp decrease in moisture of the solid phase and the increase in vapor content in the gas phase. However during the pyrolysis stage full cracking was not obtained, which is reflected in the small fraction of char generated compared to the biomass' potential (47.8% of biomass pyrolyzed). After drying and the incomplete pyrolysis, there is stagnation of the solid stage model, which is seen as the char generated instead of being converted to gas remains constant in the gasifier.

In figure 3b it is seen how the vapor after biomass drying increases considerably. Moreover, some homogenous reactions took place given that the products of pyrolysis methane and hydrogen are consumed. This indicates that oxidation reactions, at least those of homogeneous nature (R4-7), are proceeding and producing steam and carbon monoxide.

According to this simulation the maximum temperature, shown figure 4, within the gasifier was 430°C in gas phase, with a peak in solid temperature at around 267 °C. These temperatures are insufficient for complete pyrolysis and activation of the heterogeneous reactions. The temperatures reached by this model were not enough to activate the exothermic reactions that occur inside a gasifier. The low temperatures obtained by the models did not allow for the proper evolution of the gases along the different reaction zones, thus a two segment model was implemented.

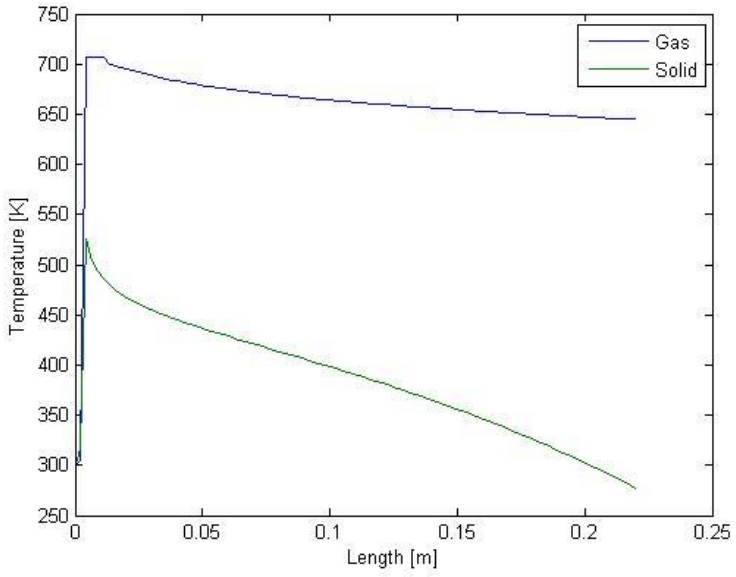

Figure 4. Axial profile of solid phase and gas phase temperatures for complete gasification

- **Drying-Pyrolysis and Oxidation-Reduction simulations**

As second test of the model, a two segment simulation was performed. The initial conditions for drying-pyrolysis segment are the same as the complete gasification simulation and the outputs obtained are used as inputs into the oxidation-reduction segment. [33] Since the boundaries are not specified in a gasification process and the stages overlap each other, the segment length is the same. The drying-pyrolysis segment was executed to establish the amount of each substance produced by biomass' cracking, subsequently, following the considerations described in Babu [33] with a normalized length to ensure the complete pyrolysis. The initial temperature of the oxidation-reduction segment was fixed as 1127 °C based on the experimental data [23] . Figure 5 depicts the route taken within the two-segment simulation.

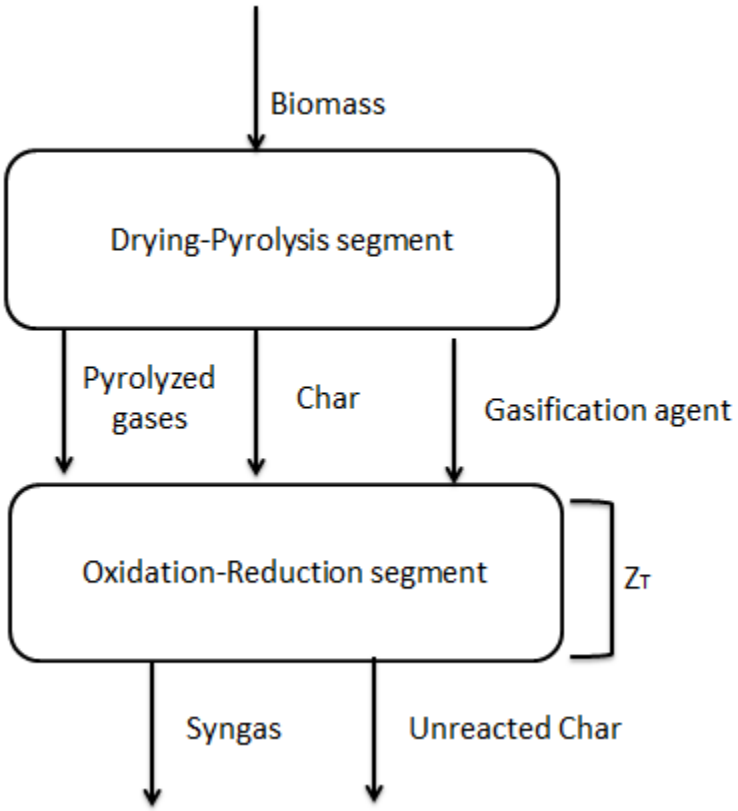

Figure 5. Two-segment simulation scheme.

Figure 6 shows the molar flow profiles of solid and gas phases, respectively, for the Drying-Pyrolysis segment. Both stages are developed completely, showing total biomass conversion into char and gas components and entire evaporation of biomass moisture.

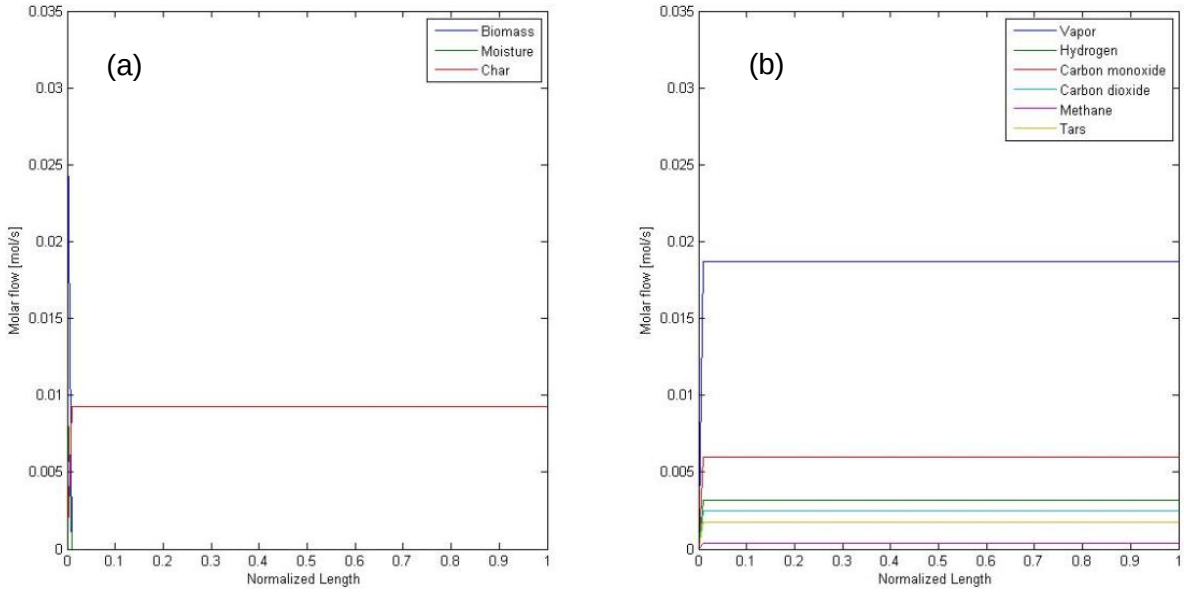

Figure 6. Axial profile of solid (a) and gas (b) species flows in drying-pyrolysis segment

In this case, the segment reaches a highest temperature (solid phase) at around 2150 °C, figure 7 shows behavior. At this point pyrolysis is completed and because pyrolysis and drying take place in the solid phase, there is almost no change in the gas temperature. After completing the biomass cracking, the results are used as inputs for oxidation-reduction. Hence, drying-pyrolysis segment acts as the kinetic conditioning, which establishes the amount of pyrolyzed gas mixture and char. The oxidation-reduction zone simulation presented partial reduction of char, as seen in figure 8. Char reaches a conversion of 90.2%. The char reaction rate is almost constant in the axial direction, as seen from the almost constant descending slope. The behavior of the gas phase species in this segment (Fig 8b) shows a large generation of steam and carbon monoxide. The reactions occur simultaneously, however they could be affected by the temperature gap between solid and gas phases, which was predicted to be over 1800°C. This has a direct influence on the kinetics of the reactions. Due to the exothermic nature of homogenous oxidation reactions, which increases the temperature of the system, and the endothermic nature of heterogeneous reduction reactions, which decrease the temperature, a thermic imbalance could be causing the temperature differences.

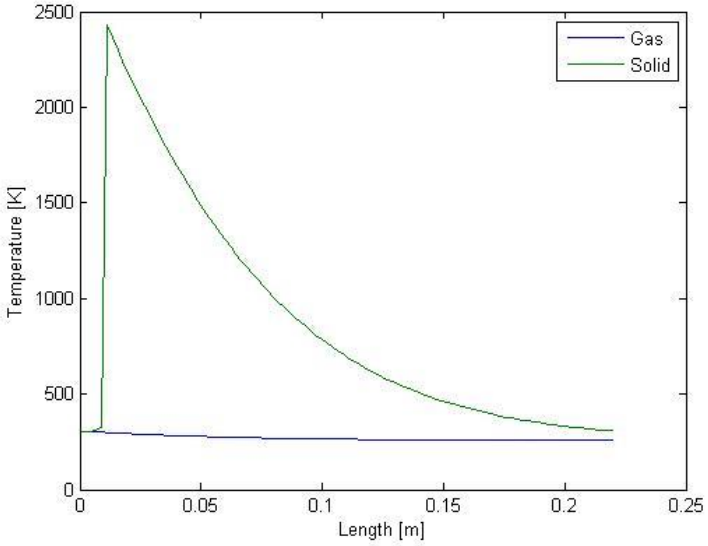

Figure 7. Axial profile of solid phase and gas phase temperatures for drying-pyrolysis segment

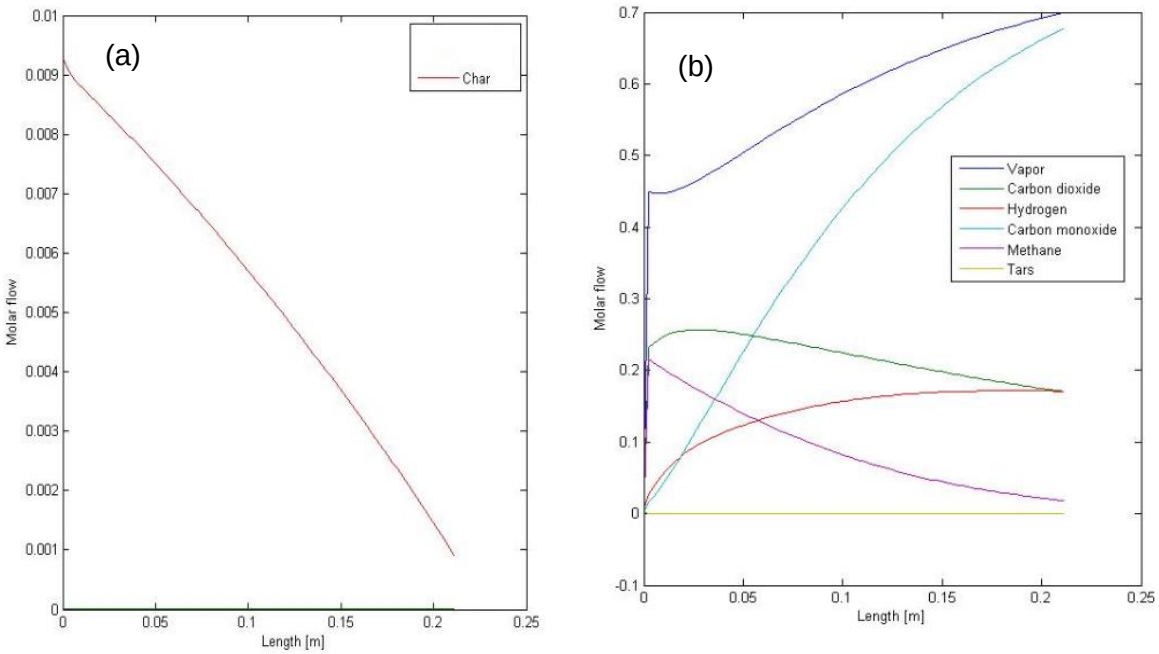

Figure 8. Axial profile of char flow (a) and gas phase species (b) in the oxidation-reduction segment.

As overview of both simulations carried out, it should be noticed that the evaporation of moisture occurs rapidly likely because the simplified model, in which inner particle temperature gradients are not considered. The results obtained in the oxidation-reduction segment are then compared to experimental results. [23] The experimental gas analysis are based in dry gas composition, therefore the results of the simulation of the outlet of the oxidation reduction segment are also taken as dry gas. The comparison with the experimental values is shown in Figure 9.

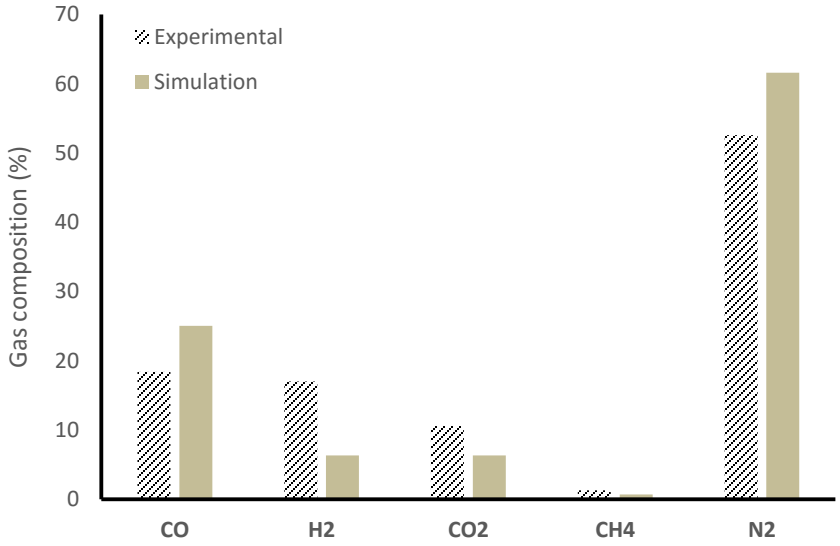

Figure 9. Validation of the simulated results to the experimental data for rubber wood. **[23]**

Based upon Fig. 9, there is a fair agreement of the simulated results to the experimental data. However, large underpredictions of hydrogen and carbon dioxide content were observed. The two-segment simulation brings a more illustrative perspective about the model performance than the full four stages simulation due to the total pyrolyzed biomass instead of the 47.8% biomass conversion. Therefore, the two-segment simulation allows for a more detailed description of the gasification stages.

The drying-pyrolysis segment, defined as a kinetic conditioning for the oxidation-reduction segment, is a convenient model adaptation to define the products of pyrolyzed biomass. The sub model by Thuman et al. [26], implemented has been validated with good results [13] and allows an adaption the fuel specifications in order to stablish char and gas mixture fractions. Moisture evaporation has a right representation of the phenomena, almost instant evaporation due to the high temperatures reached.

Although the oxidation-reduction segment did not meet complete char conversion (90.2% conversion), it gives valuable insights about the prevalence of some gas species, which are closely tied to temperature changes in a gasification process. Among the gas product:

steam and carbon monoxide amounts are significant, Fig. 9 indicates an underpredicion of 4% in carbon dioxide and 11% in hydrogen and an overpediction of 7% in carbon monoxide. These species are products and reactants of the *water gas shift reaction* (R.14), a reversible reaction with great dependence in temperature. The sensitive behavior of the *water gas shift reaction* caused an abundant production of steam and carbon monoxide due to the high gas temperatures, with concordance to Le Chatelier's principle, and a consumption of hydrogen and carbon dioxide.

The temperature, as measure of thermic energy, depicts the behavior of the model. Chemical kinetics, in this case Arrhenius type, depends on temperatures and any flaw affects the entire results. At first glance the cause of the temperatures differences suggests a failure of the model in the solid-gas convective heat transfer, possibly a decoupling between phases.. The reaction nature, either exothermic or endothermic, increases or decreases temperatures and gasification processes have both reaction natures that act simultaneously.

Section 5.9 explains the continuity equations chosen for the model with their assumptions based on section 4. The considerations taken in the energy aspects posed an exclusion of thermal conductivity phenomena. According to Souza [9], thermal conductive acts as a smoothing factor that balances abrupt changes among the reactions energy source term, in other words, this means that the second derivative, which represents thermal conductivity, has a direct influence to set a thermic equilibrium. Thus, when exothermic reactions take place, increasing temperatures, second derivatives moderates the changes acting as a dissipative term, and vice versa with endothermic reactions.

The rapid exhaustion of oxygen due to oxidation reactions, which are exothermic and increase the temperature abruptly until endothermic reactions start to occur. On the other hand with the solid temperature, the changes are not so drastic, probably due to the equilibrium among exothermic and endothermic heterogeneous reactions.

Nevertheless, it is clear the influence of the thermal conductivity in the energy conservation within a gasification process. At least in the developed model a misfit of the energy balance was observed, additionally the radiation effects were neglected within the balance affecting a source of heat transfer that represents a more realistic process. When implementing a mathematical model from literature sources, the consistency is a key step. The advisable path to follow is: sticking to a model already proposed and implement it in order to stay coherent. Then, changes and alterations to the model could be implemented once the original model is validated. The scope of this work proposes a model that, although solves the stiff DAE system, did not reach an accurate process representation of

the thermic phenomena. At a kinetic viewpoint the two simulations carried out performed according to the temperatures obtained.

8. Conclusions

A model of a downstream gasifier was developed and implemented using Matlab. The most important parameters that constituted a gasification process were determined. The chosen models were selected base on literature sources, available information fit on with the model assumptions and considerations settled in the proposal. The model was solved using ODE15s, a MATLAB subroutine suitable for stiff systems such as the gasification process.

Validation was carried out comparing the outlet compositions to experimental results available in the literature. The composition of carbon monoxide and nitrogen were overpredicted, while those of hydrogen and carbon dioxide were underpredicted.

The developed model allow for composition predictions at each gasification stage. The two-segment simulation illustrates better how the interactions between stages occur. Drying and pyrolysis stages show biomass transformation into char and gas species, setting a kinetic conditioning for the oxidation-reduction segment. In the kinetic approach the model chemical mechanism behaves as a function of the temperature of the system, which in turn also depends in the energy released or absorbed by the reactions themselves. Gasification processes have a complex chemical nature that adds difficulties for their representation in mathematical models. Consistency at the time to implement computing modeling is suggested, during the model selection, rather than using different sources, a consolidated model is advisable.

9. Properties and Nomenclature

9.1 Correlations for thermochemical properties

Table 12. Solid phase properties **[24]**

Properties	Value
Specific Heat [J/ kg K]	$C_{p,bms} = 3.86 \cdot T + 103.1$ $C_{p,H2OL} = 4180$ $C_{p,char} = 0.36 \cdot T + 1390$
Formation enthalpy [J/mol]	$h°_{f,bms} = -89854.0977$ $h°_{f,H2OL} = -285e3$ $h°_{f,char} = 0$

Table 13. Gas phase properties

Properties	Value
Specific Heat [J/ mol K]	$C_{p,tars} = 88.627 + 0.12074 \cdot T - 0.12735e\text{-}4 \cdot T^2 - 0.36688e7 / T^2$ See Table 10 for the others
Formation enthalpy [KJ/mol]	$h°_{f,i}$ = H (Table 10) $h°_{f,tars} = 82.927$
Thermal conductivity [W/m K]	$K_g = 25.77e\text{-}3$
R [J/mol K]	8.314
Viscosity [$\boldsymbol{\mu P}$]	$\mu_g = A + B \cdot T + C \cdot T^2$ See Table 11.

Table 14. Gas phase correlations (Janaf Table) **[34]**

Specie	T(K)	A	B	C	D	E	F	G	H
CO	298 < T < 1300	25.56759	6.09613	4.054656	-2.671301	0.131021	-118.0089	227.3665	-110.5271
CO_2	298 < T < 1200	24.99735	55.18696	-33.69137	7.948387	-0.136638	-403.6075	228.2431	-393.5224
H_2	298 < T < 1000	33.066178	-11.363417	11.432816	-2.772874	-0.158558	-9.980797	172.707974	0.0
CH_4	298 < T < 1300	-0.703029	108.4773	-42.52157	5.862788	0.678565	-76.84376	158.7163	-74.8731
H_2O	298 < T < 1700	30.092	6.832514	6.793435	-2.53448	0.082139	-250.881	223.3967	-241.8264
N_2	298 < T < 1300	26.092	8.218801	-1.976141	0.159274	0.044434	-7.98923	221.02	0.0
O_2	298 < T < 1200	29.659	6.137261	-1.186521	0.09578	-0.219663	-9.861391	237.948	0.0

$$C_{p,i} = A + B \cdot T + C \cdot T^2 + D \cdot T^3 + E/T^2 \ [J/mol\ k]$$

$$T = tempeture(K)/10$$

Table 15. Gas phase correlations for viscosity **[35]**

Specie	A	B	C
CO	23.811	5.39E-01	-1.54E-04
CO_2	11.811	4.98E-01	-1.09E-04
H_2	27.758	2.12E-01	-3.28E-05
CH_4	3.844	4.01E-01	-1.43E-04
H_2O	-36.826	4.29E-01	-1.62E-05
N_2	42.606	4.750E-01	-9.88e-05
O_2	44.224	5.620E-01	-1.13e-04

$$\mu_g = A + B \cdot T + C \cdot T^2 \ [\mu P]$$

9.2 Nomenclature

A	Gasifier area [m^2]
A_j	Phase area [m^2]
C	Mass fraction of carbon
$C_{char,bms}$	Initial moles of char in a biomass mole [mol/ m^3]
C_i	Molar concentration of component i [mol/m^3]
C_p	Specific heat [J/ mol K]
D_j	Diffusivity coefficient [m^2 /s]
d_p	Particle diameter [m]
d_t	Gasifier diameter [m]
E_j	Activation energy of reaction j [kJ/mol]
h_{sg}	Heat transfer coefficient by convection
$h°_{f,i}$	Formation enthalpy of specie i [J/mol]
$h_{m,j}$	Mass transfer coefficient of reaction j [m/s]
$h_{T,i}$	Enthalpy for specie i [J/mol]
H_i	Energy flow of phase i [J/s]
H	Mass fraction of hydrogen
k_c	Kinetic constant of heterogeneous reaction [m/s]
k_e	Effective reaction rate [m/s]
k_s	Thermal conductivity [W/m k]
k_j	Kinetic constant of reaction j
m	Hydrogen atoms in biomass
n	Carbon atoms in biomass
n_i	Molar flow of specie i [mol /s]
N	Mass fraction of nitrogen
Nu	Nusselt number
O	Mass fraction of oxygen
p	Oxygen atoms in biomass
Pr	Prandtl number
Q_{sg}	Solid/Gas energy transfer [W/ m^3]
$\tilde{r}_j$	Kinetic reaction rate [mol/ m^3K]
Re	Reynolds number
R	Universal gas constant [J/mol K]
Sc	Schmidt number
Sh	Sherwood number
T_i	Temperature of phase i [K]
u_j	Velocity of specie j [m/s]
W_i	Molecular weight of I [g/mol]
w	Molar fraction of moisture in biomass
ε	Void fraction
μ_g	Gas viscosity [kg/m s]
$\nu_{i,j}$	Stoichiometric coefficient of specie i in reaction j
ν_p	Density particle number [1/m]
Ω_1	Mass relation CO/CO2 pyrolyzed
Ω_2	Mass relation CH4/CO2 pyrolyzed
Ω_3	Mass relation H2O/CO2 pyrolyzed
ρ_g	Mass concentration of gas [kg/m^3]
$-\Delta H$	Reaction enthalpy kJ/mol

10. References

[1] GENI, "Renewable Energy Potential Of Latin America," Global Energy Network Institute, San Diego, 2009.

[2] World Energy Council, "Survey of Energy Resources," World Energy Council, London, 2010.

[3] T. Bhaskar and A. Pandey, "Advances in Thermochemical," in *Recent Advances in Thermochemical Conversion of Biomass*, Amsterdam, Elsevier, pp. 1-28, 2015,.

[4] P. Basu, Biomass Gasification, Pyrolysis and Torrefaction, London: Academic Press, 2013.

[5] P. Grammelis, Solid Biofuels for Energy, Athens: Springer, 2011.

[6] Y. Richardson, M. Drobek, A. Julbe and J. Blin, "Biomass Gasification to Produce Syngas," in *Recent Advances in Thermo-Chemical Conversionof Biomass*, Elsevier, pp. 213-250, 2015.

[7] R. Budhathoki, "Three zone modeling of Downdraft biomass Gasification: Equilibrium and finite Kinetic Approach," Thesis University of Jyväskylä, 2013.

[8] R. Gani and E. Pistikopoulos, "Property modelling and simulation for product and process design," *Fluid Phase Equilibria,* no. 197, pp. 43-59, 2002.

[9] M. de Souza-Santos, Solid fuels combustion and gasification : modeling, simulation, and equipment, Boca Raton: Taylor & Francis, 2010.

[10] M. Arnavat, . J. Bruno and A. Coronas, "Review and analysis of biomass gasification models," *Renewable and Sustainable Energy Reviews,* vol. 14, p. 2841–2851, 2010.

[11] D. Baruah and D. Baruah, "Modeling of biomass gasification: A review," *Renewable and Sustainable Energy Reviews,* vol. 39, pp. 806-815, 2014.

[12] P. Basu, Biomass Gasification and Pyrolysis: Practical Design and Theory, Elsevier, 2010.

[13] J. F. Pérez Bayer, Gasificación de biomasa: Estudios teórico-experimentales en lecho fijo equicorriente., Medellín: Editorial Universidad de Antioquia, 2009.

[14] U. Henriksen, . J. Ahrenfeldt, . T. Kvist and . B. Gøbel, "The design, construction and operation of a 75 kW two-stage gasifier," *Energy,* vol. 31, no. 10-11, p. 1542–1553, 2015.

[15] M. Puig-Arnavat and J. C. Bruno, "Artificial Neural Networks for," in *Recent Advances in Themochemical Conversion of Biomass*, pp. 133-155, Elsevier, 2015.

[16] J. Baxter Milligan, Downdraft Gasification of Biomass, PhD Thesis, Aston University, 1994.

[17] D. Giltrap, R. McKibbin and G. Barnes, "A steady state model of gas-char reactions in a downdraft," *Solar Energy,* vol. 74, pp. 85-91, 2003.

[18] Z. Zainal, R. Ali, C. H. Lean and K. N. Seetharamu, "Prediction of performance of a downdraft gasifier using equilibrium modeling for different biomass materials," *Energy Conversion and Management ,* vol. 42, pp. 1499-1515, 2001.

[19] B. Gøbel, U. Henriksen, T. K. Jensen, B. Qvale and N. Houbak, "The development of a computer model for a fixed bed gasifier," *Bioresource Technology ,* vol. 98, pp. 2043–2052, 2007.

[20] A. Melgar, J. Pérez, H. Laget and A. Horillo, "Thermochemical equilibrium modelling of a gasifying process," *Energy Convertion and Management,* vol. 48, pp. 59-67, 2007.

[21] A. K. Sharma, "Equilibrium and kinetic modeling of char reduction reactions," *Solar Energy,* vol. 82, pp. 918–928, 2008.

[22] I. Janajreh and M. Al Shrah, "Numerical and experimental investigation of downdraft gasification of wood chips," *Energy Conversion and Management,* vol. 65,pp.783–792, 2013.

[23] T. H. Jayah, L. Aye, R. J. Fuller and D. F. Stewart, "Computer simulation of a downdraft wood gasifer for tea drying," *Biomass and Bioenergy,* vol. 25, pp. 459-469, 2003.

[24] J. Pérez, A. Melgar and F. Tinaut, "Modeling of fixed bed downdraft biomass gasification: application on lab-scale and industrial reactors," *International Journal of Energy Research,* vol. 38, pp. 319-338, 2014.

[25] M. Arnavat, J. A. Hernandez and A. Coronas, "Artificial neuralnetwork models for biomass gasification in fluidized bed gasifiers," *Biomass Energy,* no. 49, pp. 279-289, 2013.

[26] H. Thuman, F. Niklasson , F. Johnsson and B. Leckner , "Composition of volatile gases and thermo chemical properties of wood for modeling of fixed or fluidized beds," *Energy & Fuels,* no. 15, pp. 1488–1497, 2001.

[27] K. Bryden , K. Ragland and C. Rutland , "Modeling thermally thick pyrolysis of wood," *Biomass and Bioenergy,* no. 22, pp. 41-53, 2002.

[28] C. Di Blasi, "Dynamic behaviour of stratified downdraft gasifiers," *Chemical Engineering Science,* no. 55, pp. 2931-2944, 2000.

[29] M. Seggiani, M. Puccini and S. Vitolo, "Gasification of Sewage Sludge: Mathematical," *Chemical Engineering Transactions,* vol. 32, pp. 895-900, 2013.

[30] A. Gonstantinides and N. Mostoufi, Numerical Methods for Chemical Engineers with MATLAB Applications, New Jersey : Prentice Hall , 2000.

[31] F. Bruce, Introduction to chemical engineering computing, New Jersey: John Wiley , 2012.

[32] C. Moler, Numerical Computing with MATLAB, Natick: The MathWorks, Inc., 2004.

[33] B. Babu and P. Sheth, "Modeling and simulation of reduction zone of downdraft biomass gasifier: Effect of char reactivity factor," *Energy Conversion and Management,* no. 47, p. 2602–2611, 2006.

[34] M. W. Chase, "Thermochemical Tables," *Journal Physical Chemical Reference Data,* p. monograph 9, 1998.

[35] C. L. Yaws, Chemical Properties Handbook: Physical, Thermodynamic,Environmental, Transport, Safety, and Health Related Properties for Organic and Inorganic Chemicals, McGraw-Hill, 1995.

[36] D. Giltrap, R. McKibbin and G. Barnes, "A steady state model of gas-char reactions in a downdraft," *Solar Energy,* no. 74, pp. 85-91, 2003.

APPENDIX

1. ODE15s structured code

- **Biomass treatment**.

```
function [n m p nmoi Ychar ncharC nbms wbms Cchar no2
nn2]=Biomass(Ci,Hi,Oi,moi,Br,vol,ash,pbms,ER,CF)

%%% Initial biomass treatment- biomass molecular weight- char
concentration

wC = 12;
wH = 1;
wO = 16;
wh2o = 18;
wn2=28;
wo2=32;

%moles coefficients( molecular formnula)
 n=1;
m=(Hi*wC)/(Ci*wH);
p=(Oi*wC)/(Ci*wO);

volW=vol*(1-moi);
ashW=ash*(1-moi);
CFW=CF*(1-moi);
total=volW+ashW+CFW+moi;

wbms= wC*n + wH*m +wO*p; % Biomass molecular weight
w=((wbms*moi)/(wh2o*(1-moi)));
NbmsMois = ((((Br*1000)/wbms))/3600); %  Kg/h to mol/s
nbms=NbmsMois*(1-w);
nmoi=NbmsMois*w;

Ychar = (CFW/(total))*(wbms/wC); %Initial char molar fracton
ncharC=Ychar*nbms; %initial char moles
ERst=(1+m/4-p/2)*((wo2+3.76*wn2)/wbms); %stoiquiometric equivalent ratio
ERR=ER/ERst;

no2=((1+m/4-p/2)*ER)*0.21; %oxigen flow
nn2=((1+m/4-p/2)*ER)*0.79; %nytrogen flow
Cchar = (((CFW))*(pbms/wC))*1.000; % initial molar concentration of char
within biomass
end
```

- **Matrix code.**

```
function [z,y]=gasifier(z_max)
```

```
%%% Form of the state vector [n_bms, n_water, n_char, n_o2, n_n2,
n_steam,
%%% n_co2, n_h2, n_co, n_ch4, n_tars, Hg, Hs, Tg, Ts]

global wbms
global C_char
global pbms
global ncharC
global Ychar dp dt

%% Input variables and biomass composition calculation

%%% Dimensions of the gasifier and the particles

dp=0.044; %Diameter of the particles [m]
dt=0.92;  %Diameter of the tube [m]

%%% Proximate composition analysis-moisture content-biomass
specifications

Ci = 0.506;
Hi = 0.065;
Oi = 0.42;
moi = 0.16;
Br = 3.5;
ER=1.96;
vol = 0.801;
CF=0.192;
ash = 0.007;
pbms =320000;
%%% Initial biomass treatment
[n m p n_water Ychar ncharC n_bms wbms C_char n_o2 n_n2]=
Biomass(Ci,Hi,Oi,moi,Br,vol,ash,pbms,ER,CF);

%% Entry conditions for the ODE solution


n_co=10^-6;
n_co2=10^-6;
n_steam=10^-6;
n_h2=10^-6;
n_ch4=10^-6;
n_tars=10^-6;
n_char=10^-6;
Ts=300;
Tg=300;

%Total enthalpy of the components at solid temperature
h_ts=t_enthalpy(Ts);
%Total enthalpy of the components at gas temperature
h_tg=t_enthalpy(Tg);
```

```
%Enthalpy flow of the solid stream
Hs=dot([n_bms, n_water, n_char], h_ts(1:3));

%Enthalpy flow of the gas stream
Hg=dot([n_o2, n_n2, n_steam, n_co2, n_h2, n_co, n_ch4, n_tars],
h_tg(4:11));

%Mass matrix: Temperatures calculated algebraically (iteratively)
mass=diag([1 1 1 1 1 1 1 1 1 1 1 1 1 0 0]);
%Initial conditions (entry conditions)
y0=[n_bms, n_water, n_char, n_o2, n_n2, n_steam,n_co2, n_h2, n_co, n_ch4,
n_tars, Hg, Hs, Tg, Ts]';

%%% Solution of the ODE system
options=odeset('mass',mass,'abstol',10^-6,'reltol',10^-3);
[z,y]=ode15s(@rhs,linspace(0,0.22,100),y0,options);


%% Plotting of results

plot(z,y(:,14),z,y(:,15))
legend('Gas','Solid')
xlabel('Length [m]')
ylabel('Temperature [K]')

figure
subplot(1,2,1)
plot(z,y(:,1:3))
legend('Biomass','Moisture', 'Char')
xlabel('Length [m]')
ylabel('Molar flow')

subplot(1,2,2)
plot(z,y(:,6:11))
legend('Vapor', 'Carbon dioxide', 'Hydrogen','Carbon monoxide',
'Methane', 'Tars')
xlabel('Length [m]')
ylabel('Molar flow')



function ydot=rhs(z,y)

%%
%%% Form of the state vector [n_bms, n_water, n_char, n_o2, n_n2,
n_steam,
%%% n_co2, n_h2, n_co, n_ch4, n_tars, Hg, Hs, Tg, Ts]

ydot=zeros(15,1);

global wbms
global C_char

global dp dt
```

```
%%% State variables
n_bms= y(1);
n_water=y(2);
n_char=y(3);
n_o2=y(4);
n_n2=y(5);
n_steam=y(6);
n_co2=y(7);
n_h2=y(8);
n_co=y(9);
n_ch4=y(10);
n_tars=y(11);
Hg=y(12);
Hs=y(13);
Tg=y(14);
Ts=y(15);

 %%% Stoichiometric matrix: Every row represents a species, every column
%%% represents a reaction:

nu=[0   -1  0   0   0   0   0   0   0   0   0   0   0
-1  0   0   0   0   0   0   0   0   0   0   0
0   0.299   0   0   0   0   -2  -1  -1  -1  0   0   0
0   0   -2.9    -1.5    -1  -1  -1  0   0   0   0   0   0
0   0   0   0   0   0   0   0   0   0   0   0
1   0.2577  0   2   0   2   0   0   0   -1  -1  -5.8    -1
0   0.1014  0   0   2   0   0   -1  0   0   0   0   1
0   0.1932  3.1 0   0   -2  0   0   -2  1   3   8.9 1
0   0.0798  6   1   -2  0   2   2   0   1   1   6   -1
0   0.0125  0   -1  0   0   0   0   1   0   -1  0   0
0   0.0564  -1  0   0   0   0   0   0   0   0   -1  0
];


%Dimensional parameters and conditions

e = 0.38+0.073*(1+((dt/dp)-2)^2/((dt/dp)^2)); %Bed void fraction [-]
r = dt/2;                                     %Radius of the pipe [m]
vp = (6*(1-e))/dp;                            %Specific gas-solid
interface
A_g = e*pi*r^2;                               %Free cross section of gas
flow [m2]
A_s = (1-e)*pi*r^2;                           %Free cross section of
solid flow [m2]
ll = 0.02;                                    %Factor for heat transfer
R = 8.314;                                    %Gas constant [J/mol K]
P = 101325;                                   %Pressure [Pa]
tref = 298.15;                                %Reference temperature [K]

%%% Reaction area matrix: Diagonal matrix that indicates in which phase
the
%%% reaction takes place, by assigning the corresponding cross-section to
%%% each reaction rate, i.e. for gas-solid reactions, the area is A_s
```

```
A_m=diag([A_s, A_s, A_g, A_g, A_g, A_g, A_s, A_s, A_s, A_s, A_g, A_g,
A_g]);

%Molecular weights [g/mol]
w_co2=44;
w_co=28.01;
w_ch4=16.0425;
w_h2o=18;
w_char=12;
w_h2=2;
w_n2=28;
w_o2=32;
w_tars=81.522;

%Total gas concentration
C_gas=P/(R*Tg);

%Total gas flow
n_gas=sum(y(4:11));

%Gas velocity
u_g = n_gas/(A_g*C_gas);

%Concentrations
C_h2=(n_h2/n_gas)*C_gas;
C_o2=(n_o2/n_gas)*C_gas;
C_co2=(n_co2/n_gas)*C_gas;
C_n2=(n_n2/n_gas)*C_gas;
C_steam=(n_steam/n_gas)*C_gas;
C_co=(n_co/n_gas)*C_gas;
C_ch4=(n_ch4/n_gas)*C_gas;
C_tars=(n_tars/n_gas)*C_gas;

y_char=nu(3,2);
C_bms=(n_bms*C_char)/(y_char*n_bms+n_char);
C_water=(n_water*C_char)/(y_char*n_bms+n_char);

%%% Transport data calculation: Mass and heat transfer

%Mass density of the gas phase
rho_g =
(C_o2*w_o2+C_n2*w_n2+C_h2*w_h2+C_co2*w_co2+C_co*w_co+C_ch4*w_ch4+C_tars*w
_tars+C_steam*w_h2o)/1000;

%Dynamic viscosity of the gas phase

mu_g= viscosity(Tg)

%Diffusion coefficients [m2/s]
D=[7.22e-4, 6.16e-4, 28.89e-4, 9.63e-4];

%Reynolds number
Re=rho_g*dp*u_g/mu_g;
```

```
%Schmidt numbers
Sc=mu_g./(rho_g.*D);

%Sherwood numbers
Sh=0.9*(2+0.6*Re^0.6*Sc.^(1/3));

% Mass diffusion coefficients for the heterogenuos reactions
hm=Sh.*D/dp; %[h_mc5, h_mg1, h_mg2, h_mg3]

%Heat transfer coefficient and heat transfer between gas-solid

h_sg= coefsg(ug,cpgm,Pg,dp,vg);
Q_sg=ll*h_sg*vp*(Ts-Tg);

%%% Reaction data

%Reaction rates
r_rate=kinetics (C_bms, C_water, C_char, C_o2, C_n2, C_steam, C_co2,
C_h2, C_co, C_ch4, C_tars, Tg, Ts, P, hm, vp, w_char, w_o2, w_co2,
w_h2,w_h2o);

%Total enthalpy of the components at solid temperature
h_ts=t_enthalpy(Ts);

%Total enthalpy of the components at gas temperature
h_tg=t_enthalpy(Tg);
%Formation Enthalpies
hfco=-110.5271*1000;
hfco2=-393.5224*1000;
hfch4=-74.87310*1000;
hfh2o=-241.8264*1000;
hftars=82.927*1000;


% Heat of reactions
vc1=6*hfco-hftars;
vc2=(hfco+2*hfh2o)-hfch4;
vc3=2*hfco2-2*hfco;
vc4=2*hfh2o;
vc5=2*hfco;
vg1=2*hfco-hfco2;
vg2=hfch4;
vg3=hfco-hfh2o;
vg4=hfco-(hfh2o+hfch4);
vg5=6*hfco-(5.8*hfh2o+hftars);
vwg=hfco2-(hfco+hfh2o);

%Heat exchange due to mass transfer (source term)

Q_s=A_s*(r_rate(1)*(434730.6)+r_rate(7)*(-vc5)+r_rate(9)*(-
vg2)+r_rate(8)*(-vg1)+r_rate(10)*(-vg3));
```

```
Q_g=A_g*(r_rate(3)*(-vc1)+r_rate(11)*(-vg4)+r_rate(6)*(-vc4)+r_rate(4)*(-
vc2)+r_rate(5)*(-vc3)+r_rate(13)*(-vwg)+r_rate(12)*(-vg5));

%% Setup of actual ODE system: mass and energy balances

%%% Order of the components [bms, water, char, o2, n2, steam,co2, h2, co,
ch4, tars]
%%%% Order of reactions: [rd, rp, rc1, rc2, rc3, rc4, rc5, rg1, rg2, rg3,
rg4, rg5, rwg]

%%% Balances for the species: Convection=reaction

ydot(1:11,1)=nu*A_m*r_rate;

%%% Energy balances

%Energy balance of the gas phase
ydot(12) = -A_s*Q_sg-Q_g;

%Energy balance of the solid phase
ydot(13) = -A_s*Q_sg+Q_s;

%Residual for the calculation of the temperature of the gas
ydot(14) = Hg-dot(y(4:11),h_tg(4:11));

%Residual for the calculation of the temperature of the solid
ydot(15) = Hs-dot(y(1:3),h_ts(1:3));
```

- **Enthalpy estimation.**

```
function h_t=t_enthalpy(T)

%%%% Vector containing the total enthalpy of each species at a specified
%%%% temperature

T_ref=298.15;

h_t=zeros(11,1);

%%% Order of the components [bms, water, char, o2, n2, steam,
%%% co2, h2, co, ch4, tars]



%Cp of the gases: [O2, N2, steam, CO2, H2, CO, CH4, tars]
%Form of the eq: Cp=A+Bt+Ct^2+Dt^3+E/t^2; t=T/1000

%Gases in this cp matrix and formation enthalpy vector: O2, N2, steam,
CO2,
%H2, CO, CH4]
Cp=[29.659 6.137261 -1.186521 0.095780 -0.219663 -9.861391 237.9480 0.0
```

```
    26.09200 8.218801 -1.976141 0.159274 0.044434 -7.989230 221.0200 0.0
    30.09200 6.832514 6.793435 -2.534480 0.082139 -250.8810 223.3967 -
241.8264
    24.99735 55.18696 -33.69137 7.948387 -0.136638 -403.6075 228.2431 -
393.5224
    33.066178 -11.363417 11.432816 -2.772874 -0.158558 -9.980797
172.707974 0.0
    25.56759 6.096130 4.054656 -2.671301 0.131021 -118.0089 227.3665 -
110.5271
    -0.703029 108.4773 -42.52157 5.862788 0.678565 -76.84376 158.7163 -
74.87310
    ]; %[j/mol k]

hf=1000*[0; 0; -241.83; -393.51; 0; -110.53; -74.87]; %[j/mol]

%%% Calculation of the enthalpy for the gaseous components
t=T/1000;
t_ref=T_ref/1000;

h_t(4:10)=hf+1000*(Cp(:,1)*(t-t_ref)+Cp(:,2)*(t^2-
t_ref^2)/2+Cp(:,3)*(t^3-t_ref^3)/3+Cp(:,4)*(t^4-
t_ref^4)/4+Cp(:,5)*(1/t_ref-1/t));

%%% Calculation for the biomass

w_bms=23.5020; %[g/mol]
h_t(1)=-89854.0977+(w_bms/1000)*(3.86*(T^2-T_ref^2)/2+103.1*(T-T_ref));

%%% Calculation for water

h_t(2)=-285800+(18/1000)*4180*(T-T_ref);


%%% Calculation for char

h_t(3)=0+(12/1000)*(0.36*(T^2-T_ref^2)/2+1390*(T-T_ref));

%%% Calculation for tars

h_t(11)=1000*82.927+(88.627*(T-T_ref)+0.12074*(T^2-T_ref^2)/2-0.12735e-
4*(T^3-T_ref^3)/3-0.36688e7*(1/T_ref-1/T));
```

- **Chemical Kinetics**

```
function r=kinetics(c_bms, c_water, c_char, c_o2, c_n2, c_steam, c_co2,
c_h2, c_co, c_ch4, c_tars, Tg, Ts, P, hm, vp, w_char, w_o2, w_co2,
w_h2,w_h2o)

%Returns a vector with the reaction rates

%Order of reactions: [rd, rp, rc1, rc2, rc3, rc4, rc5, rg1, rg2, rg3,
rg4,
%rg5, rwg]
```

```
r=zeros(13,1);

R=8.314; %[J/mol K]

%Calculation of the rate constants

k_d=5.13e10*exp(-88*1000/(R*Ts));
k_p1=1.44e4*exp(-88.6*1000/(R*Ts));
k_p2=4.13e6*exp(-112.7*1000/(R*Ts));
k_p3=7.38e5*exp(-106.5*1000/(R*Ts));
k_c1=59.8*exp(-101.43*1000/(R*Tg))/sqrt(1000);
k_c2=9.2e6*exp(-80.23*1000/(R*Tg));
k_c3=10^17.6*exp(-166.28*1000/(R*Tg));
k_c4=1e11*exp((-42*1000)/(R*Tg));
k_c5=1.7*Ts*exp(-74.83*1000/(R*Ts));
k_g1=3.42*Ts*exp(-129.7*1000/(R*Ts));
k_g2=1e-3*k_g1;
k_g3=1.67*k_g1;
k_g4=3015*exp(-125.52*1000/(R*Tg));
k_g5=70*exp(-16.736*1000/(R*Tg));
k_wg=2.78*exp(-12.6*1000/(R*Tg));
k_wg_e=0.0265*exp(-32.9*1000/(R*Tg));

%Mass diffusion coefficients

h_mc5=hm(1);
h_mg1=hm(2);
h_mg2=hm(3);
h_mg3=hm(3);

%Final calculation of the reaction rates

r(1)=k_d*c_water;
r(2)=(k_p1+k_p2+k_p3)*c_bms;
r(3)=k_c1*Tg*P^0.3*c_bms^0.5*c_o2;
r(4)=k_c2*Tg*c_ch4^0.5*c_o2;
r(5)=k_c3*c_co*c_o2^0.25*c_steam^0.5;
r(6)=k_c4*c_h2*c_o2;
r(7)=2*(w_char/w_o2)*vp*(k_c5*h_mc5/(k_c5+h_mc5))*c_o2;
r(8)=(w_char/w_co2)*vp*(k_g1*h_mg1/(k_g1+h_mg1))*c_co2;
r(9)=0.5*(w_char/w_h2)*vp*(k_g2*h_mg2/(k_g2+h_mg2))*c_h2;
r(10)=(w_char/w_h2o)*vp*(k_g3*h_mg3/(k_g3+h_mg3))*c_steam;
r(11)=k_g4*c_ch4*c_steam;
r(12)=k_g5*c_tars^0.25*c_steam^1.25;
r(13)=k_wg*(c_co*c_steam-c_co2*c_h2/k_wg_e);
r=real(r);
```

- **Dynamic viscosity**

```
function vg= viscosity(Tg)


%Dynamic viscosity  Tg=K, u= microPoise   to  kg/m/s
```

```
coe=[23.811 5.3944e-01 -1.5411e-04
    11.811 4.9838e-01 -1.0851e-04
    27.758 2.1200e-01 -3.2800e-05
    3.844 4.0112e-01 -1.4303e-04
    -36.826 4.2900e-01 -1.6200e-05];
uco=(coe(1,1) + coe(1,2)*Tg + coe(1,3)*Tg^2)*1e-7;
uco2=(coe(2,1) + coe(2,2)*Tg + coe(2,3)*Tg^2)*1e-7;
uh2=(coe(3,1) + coe(3,2)*Tg + coe(3,3)*Tg^2)*1e-7;
uch4=(coe(4,1) + coe(4,2)*Tg + coe(4,3)*Tg^2)*1e-7;
uh2o=(coe(5,1) + coe(5,2)*Tg + coe(5,3)*Tg^2)*1e-7;

vg = uco*xco + uco2*xco2 + uh2*xh2 + uch4*xch4 + uh2o*xh2o;
```

2. RK4 solution method and linear coding

- **RK4 solution method**

```
function q =
gasi(aa,bb,cc,gg,dd,ee,hh,ff,ii,jj,qq,nbms,nco,nco2,nh2ov,nh2,nch4,ntars,
nmoi,nchar,Hs,Hg,z,h)

global as
global rp


A1=h*eval('aa(z,nbms,nco,nco2,nh2ov,nh2,nch4,ntars,nmoi,nchar,Hs,Hg)');
B1=h*eval('bb(z,nbms,nco,nco2,nh2ov,nh2,nch4,ntars,nmoi,nchar,Hs,Hg)');
C1=h*eval('cc(z,nbms,nco,nco2,nh2ov,nh2,nch4,ntars,nmoi,nchar,Hs,Hg)');
G1=h*eval('gg(z,nbms,nco,nco2,nh2ov,nh2,nch4,ntars,nmoi,nchar,Hs,Hg)');
D1=h*eval('dd(z,nbms,nco,nco2,nh2ov,nh2,nch4,ntars,nmoi,nchar,Hs,Hg)');
E1=h*eval('ee(z,nbms,nco,nco2,nh2ov,nh2,nch4,ntars,nmoi,nchar,Hs,Hg)');
H1=h*eval('hh(z,nbms,nco,nco2,nh2ov,nh2,nch4,ntars,nmoi,nchar,Hs,Hg)');
F1=h*eval('ff(z,nbms,nco,nco2,nh2ov,nh2,nch4,ntars,nmoi,nchar,Hs,Hg)');
I1=h*eval('ii(z,nbms,nco,nco2,nh2ov,nh2,nch4,ntars,nmoi,nchar,Hs,Hg)');
J1=h*eval('jj(z,nbms,nco,nco2,nh2ov,nh2,nch4,ntars,nmoi,nchar,Hs,Hg)');
Q1=h*eval('qq(z,nbms,nco,nco2,nh2ov,nh2,nch4,ntars,nmoi,nchar,Hs,Hg)');


A2=h*eval('aa(z+h/2,nbms+A1/2,nco+B1/2,nco2+C1/2,nh2ov+G1/2,nh2+D1/2,nch4
+E1/2,ntars+H1/2,nmoi+F1/2,nchar+I1/2,Hs+J1/2,Hg+Q1/2)');
B2=h*eval('bb(z+h/2,nbms+A1/2,nco+B1/2,nco2+C1/2,nh2ov+G1/2,nh2+D1/2,nch4
+E1/2,ntars+H1/2,nmoi+F1/2,nchar+I1/2,Hs+J1/2,Hg+Q1/2)');
C2=h*eval('cc(z+h/2,nbms+A1/2,nco+B1/2,nco2+C1/2,nh2ov+G1/2,nh2+D1/2,nch4
+E1/2,ntars+H1/2,nmoi+F1/2,nchar+I1/2,Hs+J1/2,Hg+Q1/2)');
```

```
G2=h*eval('gg(z+h/2,nbms+A1/2,nco+B1/2,nco2+C1/2,nh2ov+G1/2,nh2+D1/2,nch4
+E1/2,ntars+H1/2,nmoi+F1/2,nchar+I1/2,Hs+J1/2,Hg+Q1/2)');
D2=h*eval('dd(z+h/2,nbms+A1/2,nco+B1/2,nco2+C1/2,nh2ov+G1/2,nh2+D1/2,nch4
+E1/2,ntars+H1/2,nmoi+F1/2,nchar+I1/2,Hs+J1/2,Hg+Q1/2)');
E2=h*eval('ee(z+h/2,nbms+A1/2,nco+B1/2,nco2+C1/2,nh2ov+G1/2,nh2+D1/2,nch4
+E1/2,ntars+H1/2,nmoi+F1/2,nchar+I1/2,Hs+J1/2,Hg+Q1/2)');
H2=h*eval('hh(z+h/2,nbms+A1/2,nco+B1/2,nco2+C1/2,nh2ov+G1/2,nh2+D1/2,nch4
+E1/2,ntars+H1/2,nmoi+F1/2,nchar+I1/2,Hs+J1/2,Hg+Q1/2)');
F2=h*eval('ff(z+h/2,nbms+A1/2,nco+B1/2,nco2+C1/2,nh2ov+G1/2,nh2+D1/2,nch4
+E1/2,ntars+H1/2,nmoi+F1/2,nchar+I1/2,Hs+J1/2,Hg+Q1/2)');
I2=h*eval('ii(z+h/2,nbms+A1/2,nco+B1/2,nco2+C1/2,nh2ov+G1/2,nh2+D1/2,nch4
+E1/2,ntars+H1/2,nmoi+F1/2,nchar+I1/2,Hs+J1/2,Hg+Q1/2)');
J2=h*eval('jj(z+h/2,nbms+A1/2,nco+B1/2,nco2+C1/2,nh2ov+G1/2,nh2+D1/2,nch4
+E1/2,ntars+H1/2,nmoi+F1/2,nchar+I1/2,Hs+J1/2,Hg+Q1/2)');
Q2=h*eval('qq(z+h/2,nbms+A1/2,nco+B1/2,nco2+C1/2,nh2ov+G1/2,nh2+D1/2,nch4
+E1/2,ntars+H1/2,nmoi+F1/2,nchar+I1/2,Hs+J1/2,Hg+Q1/2)');


A3=h*eval('aa(z+h/2,nbms+A2/2,nco+B2/2,nco2+C2/2,nh2ov+G2/2,nh2+D2/2,nch4
+E2/2,ntars+H2/2,nmoi+F2/2,nchar+I2/2,Hs+J2/2,Hg+Q2/2)');
B3=h*eval('bb(z+h/2,nbms+A2/2,nco+B2/2,nco2+C2/2,nh2ov+G2/2,nh2+D2/2,nch4
+E2/2,ntars+H2/2,nmoi+F2/2,nchar+I2/2,Hs+J2/2,Hg+Q2/2)');
C3=h*eval('cc(z+h/2,nbms+A2/2,nco+B2/2,nco2+C2/2,nh2ov+G2/2,nh2+D2/2,nch4
+E2/2,ntars+H2/2,nmoi+F2/2,nchar+I2/2,Hs+J2/2,Hg+Q2/2)');
G3=h*eval('gg(z+h/2,nbms+A2/2,nco+B2/2,nco2+C2/2,nh2ov+G2/2,nh2+D2/2,nch4
+E2/2,ntars+H2/2,nmoi+F2/2,nchar+I2/2,Hs+J2/2,Hg+Q2/2)');
D3=h*eval('dd(z+h/2,nbms+A2/2,nco+B2/2,nco2+C2/2,nh2ov+G2/2,nh2+D2/2,nch4
+E2/2,ntars+H2/2,nmoi+F2/2,nchar+I2/2,Hs+J2/2,Hg+Q2/2)');
E3=h*eval('ee(z+h/2,nbms+A2/2,nco+B2/2,nco2+C2/2,nh2ov+G2/2,nh2+D2/2,nch4
+E2/2,ntars+H2/2,nmoi+F2/2,nchar+I2/2,Hs+J2/2,Hg+Q2/2)');
H3=h*eval('hh(z+h/2,nbms+A2/2,nco+B2/2,nco2+C2/2,nh2ov+G2/2,nh2+D2/2,nch4
+E2/2,ntars+H2/2,nmoi+F2/2,nchar+I2/2,Hs+J2/2,Hg+Q2/2)');
F3=h*eval('ff(z+h/2,nbms+A2/2,nco+B2/2,nco2+C2/2,nh2ov+G2/2,nh2+D2/2,nch4
+E2/2,ntars+H2/2,nmoi+F2/2,nchar+I2/2,Hs+J2/2,Hg+Q2/2)');
I3=h*eval('ii(z+h/2,nbms+A2/2,nco+B2/2,nco2+C2/2,nh2ov+G2/2,nh2+D2/2,nch4
+E2/2,ntars+H2/2,nmoi+F2/2,nchar+I2/2,Hs+J2/2,Hg+Q2/2)');
J3=h*eval('jj(z+h/2,nbms+A2/2,nco+B2/2,nco2+C2/2,nh2ov+G2/2,nh2+D2/2,nch4
+E2/2,ntars+H2/2,nmoi+F2/2,nchar+I2/2,Hs+J2/2,Hg+Q2/2)');
Q3=h*eval('qq(z+h/2,nbms+A2/2,nco+B2/2,nco2+C2/2,nh2ov+G2/2,nh2+D2/2,nch4
+E2/2,ntars+H2/2,nmoi+F2/2,nchar+I2/2,Hs+J2/2,Hg+Q2/2)');


A4=h*eval('aa(z+h,nbms+A3,nco+B3,nco2+C3,nh2ov+G3,nh2+D3,nch4+E3,ntars+H3
,nmoi+F3,nchar+I3,Hs+J3,Hg+Q3)');
B4=h*eval('bb(z+h,nbms+A3,nco+B3,nco2+C3,nh2ov+G3,nh2+D3,nch4+E3,ntars+H3
,nmoi+F3,nchar+I3,Hs+J3,Hg+Q3)');
C4=h*eval('cc(z+h,nbms+A3,nco+B3,nco2+C3,nh2ov+G3,nh2+D3,nch4+E3,ntars+H3
,nmoi+F3,nchar+I3,Hs+J3,Hg+Q3)');
G4=h*eval('gg(z+h,nbms+A3,nco+B3,nco2+C3,nh2ov+G3,nh2+D3,nch4+E3,ntars+H3
,nmoi+F3,nchar+I3,Hs+J3,Hg+Q3)');
D4=h*eval('dd(z+h,nbms+A3,nco+B3,nco2+C3,nh2ov+G3,nh2+D3,nch4+E3,ntars+H3
,nmoi+F3,nchar+I3,Hs+J3,Hg+Q3)');
E4=h*eval('ee(z+h,nbms+A3,nco+B3,nco2+C3,nh2ov+G3,nh2+D3,nch4+E3,ntars+H3
,nmoi+F3,nchar+I3,Hs+J3,Hg+Q3)');
H4=h*eval('hh(z+h,nbms+A3,nco+B3,nco2+C3,nh2ov+G3,nh2+D3,nch4+E3,ntars+H3
,nmoi+F3,nchar+I3,Hs+J3,Hg+Q3)');
```

```
F4=h*eval('ff(z+h,nbms+A3,nco+B3,nco2+C3,nh2ov+G3,nh2+D3,nch4+E3,ntars+H3
,nmoi+F3,nchar+I3,Hs+J3,Hg+Q3)');
I4=h*eval('ii(z+h,nbms+A3,nco+B3,nco2+C3,nh2ov+G3,nh2+D3,nch4+E3,ntars+H3
,nmoi+F3,nchar+I3,Hs+J3,Hg+Q3)');
J4=h*eval('jj(z+h,nbms+A3,nco+B3,nco2+C3,nh2ov+G3,nh2+D3,nch4+E3,ntars+H3
,nmoi+F3,nchar+I3,Hs+J3,Hg+Q3)');
Q4=h*eval('qq(z+h,nbms+A3,nco+B3,nco2+C3,nh2ov+G3,nh2+D3,nch4+E3,ntars+H3
,nmoi+F3,nchar+I3,Hs+J3,Hg+Q3)');

nbms1=nbms+(1/6)*(A1+2*A2+2*A3+A4);
nco1=nco+(1/6)*(B1+2*B2+2*B3+B4);
nco21=nco2+(1/6)*(C1+2*C2+2+C3+C4);
nh2ov1=nh2ov+(1/6)*(G1+2*G2+2*G3+G4);
nh21=nh2+(1/6)*(D1+2*D2+2*D3+D4);
nch41=nch4+(1/6)*(E1+2*E2+2*E3+E4);
ntars1=ntars+(1/6)*(H1+2*H2+2*H3+H4);
nmoi1=nmoi+(1/6)*(F1+2*F2+2*F3+F4);
nchar1=nchar+(1/6)*(I1+2*I2+2*I3+I4);
Hs1=Hs+(1/6)*(J1+2*J2+2*J3+J4);
Hg1=Hg+(1/6)*(Q1+2*Q2+2*Q3+Q4);

q = [nbms1,nco1,nco21,nh2ov1,nh21,nch41,ntars1,nmoi1,nchar1,Hs1,Hg1];
```

- **Linear coding**

```
function [z,y]=gasiPBueno1
global wbms
global Cchar
global pbms
global ncharC
global Ychar

Ci = 0.506; %input('%wt  C biomass'); % Biomass analysis C
Hi = 0.065; %input('%wt  H biomass'); % Biomass analysis H
Oi = 0.42; %input('%wt  O biomass'); % Biomass analysis O
moi = 0.16; %input('%humedad relativa'); % Biomass %moisture
Br = 3.5; %input('Biomass rate kg/h'); % Biomass rate kg/h
ER=2.2; %input('Equivalent Ratio');
vol = 0.801; %input('%volative matter in Biomass'); % %Volative matter in
Biomass
```

```
CF=0.192;%input('%carbon fixed in Biomass'); % %carbon fixed in Biomass
ash = 0.007; %input('%ash in Biomass'); % ash in Biomass
pbms =320000; %input('Biomass specific density (kg/m3)'); % Biomass
specific density

[n m p nmoi Ychar ncharC nbms wbms Cchar no2 nn2]=
Biomass(Ci,Hi,Oi,moi,Br,vol,ash,pbms,ER,CF);

%[vco2 vco vch4 vtars vh2 vh2o ychar]=
pyrolysis(wbms,moi,ash,vol,n,m,p,CF)

nco=0;
nco2=0;
nh2ov=0;
nh2=0;
nch4=0;
ntars=0;
nchar=0;
Ts=350;
Tg=350;
tref=298.15;
Hs=nmoi*En_CPSO(Ts,'moi')+nbms*En_CPSO(Ts,'bms')+nchar*En_CPSO(Ts,'char')
;

Hg=
no2*En_Ch(Tg,'o2')+nn2*En_Ch(Tg,'n2')+nco*En_Ch(Tg,'co')+nco2*En_Ch(Tg,'c
o2')+nh2ov*En_Ch(Tg,'h2o')+nh2*En_Ch(Tg,'h2')+nch4*En_Ch(Tg,'ch4')...
    +ntars*En_CPSO(Tg,'tars');

%rutine solution
mass=diag([1 1 1 1 1 1 1 1 1 1 1 1 0 0]);

y0=[nbms,nco,nco2,nh2ov,nh2,nch4,ntars,nmoi,nchar,Hs,Hg,nn2,no2,Ts,Tg]';
%options=odeset('mass',mass);
options=odeset('mass',mass,'abstol',10^-6,'reltol',10^-6);
[z,y]=ode15s(@rhs,linspace(0,0.3,50),y0,options);

plot(z,y(:,4),'r')
axis([0,0.02,0,0.021])
xlabel('z[m]')
ylabel('Molar Flow [mol/s]')

hold on
plot(z,y(:,2),'g')
plot(z,y(:,3),'b')
plot(z,y(:,5),'c')
plot(z,y(:,6),'m')
plot(z,y(:,7),'y')
plot(z,y(:,8),'-.k')
plot(z,y(:,9),'--r')
legend('h2ov','co','co2','h2','ch4','tars','moi','char',-1)
hold off


figure
```

```
plot(z,y(:,14),'r')
axis([0,0.03,0,2000])
xlabel('z[m]')
ylabel('Ts [K]')



function ydot=rhs(z,y)

global wbms
global Cchar
global pbms
global ncharC
global Ychar


%State variables
nbms= y(1);
nco=y(2);
nco2=y(3);
nh2ov=y(4);
nh2=y(5);
nch4=y(6);
ntars=y(7);
nmoi=y(8);
nchar=y(9);
Hs=y(10);
Hg=y(11);
nn2=y(12);
no2=y(13);
Ts=y(14);
Tg=y(15);

%Dimensional parameters and conditions
dp=0.045; %m
dt=0.92; %m
e=0.38+0.073*(1+((dt/dp)-2)^2/((dt/dp)^2));
r=dt/2;
vp=(6*(1-e))/dp;
ag=e*(pi*r*r);
as=(1-e)*(pi*r*r);
ll=0.02;
R = 8.314; % J/mol/K
Pre=101325; %Pa
tref=298.15;

%Molecular weights
wco2=44;
wco=28.01;
wch4=16.0425;
wh2o=18;
wchar=12;
wh2=2;
wn2=28;
```

```
wo2=32;
wtars=81.522;

%stoichiometric pyrolisis coefficients
vco2=0.1014;
vco=0.0798;
vch4=0.0125;
vtars=0.0564;
vh2=0.1932;
vh2o=0.2577;
ychar=0.299;

%Molar frations
Cgas=Pre/(R*Tg);
ngas=no2+nn2+nh2ov+nh2+nco2+nco+nch4+ntars;
ug = ngas/(ag*Cgas);
xo2=no2/ngas;
Co2=no2/(ag*ug);
xn2=nn2/ngas;
Cn2=nn2/(ag*ug);
xh2ov=nh2ov/ngas;
Ch2ov=nh2ov/(ag*ug);
xh2=nh2/ngas;
Ch2=nh2/(ag*ug);
xco2=nco2/ngas;
Cco2=nco2/(ag*ug);
xco=nco/ngas;
Cco=nco/(ag*ug);
xch4=nch4/ngas;
Cch4=nch4/(ag*ug);
xtars=ntars/ngas;
Ctars=ntars/(ag*ug);
%Cbms=pbms/wbms;
Cbms=(nbms*Cchar)/(ychar*nbms+nchar);
Cmoi=(nmoi*Cchar)/(ychar*nbms+nchar);
%Heat coefficient

Pg=
(Co2*wo2+Cn2*wn2+Ch2*wh2+Cco2*wco2+Cco*wco+Cch4*wch4+Ctars*wtars+Ch2ov*wh
2o)/1000;
vg=viscosity(Tg);
hsg=coefsg(ug,cpgm,Pg,dp,vg);




%Formation Enthalpies
hfco=-110.5271*1000;
hfco2=-393.5224*1000;
hfch4=-74.87310*1000;
hfh2o=-241.8264*1000;
hftars=82.927*1000;
%hfh2ov= hfgvap(Tg);
hfh2ov=40.65*1000;
hfmoi=-285.3e3;
hfbms=-89854.0977;
```

```
hf=(19600+(1/wbms)*(hfco2+(1.5415)*(-285800)))*wbms;
%hfbms=(19600*wbms)+vco2*hfco2+hfco*vco+hfch4*vch4+vtars*hftars+hfh2o*vh2
o;

%Kinetics rates constants
rp=kinetics(Ts,pbms,wbms);
Kd=kineticD(Ts);
kc1 = ((59.8*1000) * exp(-(101.43*1000)/(R*Tg)));
kc2 = (9.2e6 * exp(-(80.23*1000)/(R*Tg)));
kc3 = (10^17.6 * exp(-(166.28*1000)/(R*Tg)));
kc4 = (1e11 * exp(-(42*1000)/(R*Tg)));
%kc5 = ((5.67e9) * exp(-(74.83*1000)/(R*Ts)));
kc5 = (((1.7*Ts)) * exp(-(74.83*1000)/(R*Ts)));
kg1 = (((3.42*Ts)) * exp(-(129.7*1000)/(R*Ts)));
kg2 = (((1e-3*kg1)) * exp(-(129.7*1000)/(R*Ts)));
kg3 = (((1.67*kg1)) * exp(-(129.7*1000)/(R*Ts)));
kg4 = (3015 * exp(-(125.52*1000)/(R*Tg)));

%heterogenuos reactions
hmc5=((0.9*(2+0.6*((Pg*dp*ug)/vg)^0.6*(vg/(Pg*7.22e-
4))^(0.3333)))*(7.22e-4))/dp;
hmg1=((0.9*(2+0.6*((Pg*dp*ug)/vg)^0.6*(vg/(Pg*6.16e-4))^(1/3)))*(6.16e-
4))/dp;
hmg2=((0.9*(2+0.6*((Pg*dp*ug)/vg)^0.6*(vg/(Pg*28.89e-4))^(1/3)))*(28.89e-
4))/dp;
hmg3=((0.9*(2+0.6*((Pg*dp*ug)/vg)^0.6*(vg/(Pg*9.63e-4))^(1/3)))*(9.63e-
4))/dp;

vrp=(vco2*hfco2+vco*hfco+vch4*hfch4+vtars*hftars+vh2o*hfh2o)-(hfbms);
vc1=6*hfco-hftars;
vc2=(hfco+2*hfh2o)-hfch4;
vc3=2*hfco2-2*hfco;
vc4=2*hfh2o;
vc5=2*hfco;
vg1=2*hfco-hfco2;
vg2=hfch4;
vg3=hfco-hfh2o;
vg4=hfco-(hfh2o+hfch4);

ydot(1) = -(as)*rp*Cbms;

ydot(2) =
(as)*vco*rp*(Cbms)+(as*2*2*(wchar/wo2)*vp*((kc5*hmc5)/(kc5+hmc5))*(Co2))+
(ag*6*kc1*Tg*Pre^0.3*Ctars^0.5*Co2)+(ag*kc2*Tg*Cch4^0.5*Co2)...
 -
(ag*2*kc3*Tg*Cco*Co2^0.25*Ch2ov^0.5)+(ag*1*kg4*Cch4*Ch2ov)+(as*2*(wchar/w
co2)*vp*((kg1*hmg1)/(kg1+hmg1))*(Cco2))...
 +((as)*1*(wchar/wh2o)*vp*((kg3*hmg3)/(kg3+hmg3))*(Ch2ov));

ydot(3) = (as)*vco2*rp*(Cbms)+(ag*2*kc3*Tg*Cco*Co2^0.25*Ch2ov^0.5)-
(as*(wchar/wco2)*vp*((kg1*hmg1)/(kg1+hmg1))*(Cco2));

ydot(4) =
(as)*Kd*(Cmoi)+(as)*rp*vh2o*(Cbms)+(ag*2*kc2*Tg*Cch4^0.5*Co2)+(ag*2*kc4*C
h2*Co2)-(ag*1*kg4*Cch4*Ch2ov)...
 -((as)*1*(wchar/wh2o)*vp*((kg3*hmg3)/(kg3+hmg3))*(Ch2ov));
```

```
ydot(5) = (as)*vh2*rp*(Cbms)+(ag*3.1*kc1*Tg*Pre^0.3*Ctars^0.5*Co2)-
(ag*2*kc4*Ch2*Co2)+(ag*3*kg4*Cch4*Ch2ov)-
((as)*2*0.5*(wchar/wh2)*vp*((kg2*hmg2)/(kg2+hmg2))*(Ch2))...
+((as)*1*(wchar/wh2o)*vp*((kg3*hmg3)/(kg3+hmg3))*(Ch2ov));

ydot(6) =(as)*vch4*rp*(Cbms)-(ag*kc2*Tg*Cch4^0.5*Co2)-
(ag*1*kg4*Cch4*Ch2ov)+((as)*2*0.5*(wchar/wh2)*vp*((kg2*hmg2)/(kg2+hmg2))*
(Ch2));

ydot(7) = (as)*vtars*rp*(Cbms)-(ag*1*kc1*Tg*Pre^0.3*Ctars^0.5*Co2);

ydot(8) = -(as)*Kd*(Cmoi);

ydot(9) = (as)*(ychar*rp*(Cbms))-
(as*2*2*(wchar/wo2)*vp*((kc5*hmc5)/(kc5+hmc5))*(Co2))-
(as*(wchar/wco2)*vp*((kg1*hmg1)/(kg1+hmg1))*(Cco2))...
-((as)*1*0.5*(wchar/wh2)*vp*((kg2*hmg2)/(kg2+hmg2))*(Ch2))-
((as)*1*(wchar/wh2o)*vp*((kg3*hmg3)/(kg3+hmg3))*(Ch2ov));

ydot(10) = -0.1*(pi*r*r)*(ll*hsg*vp*(Ts-
Tg))+(as)*Kd*(Cmoi)*(43473.6)+(as*1*2*(wchar/wo2)*vp*((kc5*hmc5)/(kc5+hmc
5))*(Co2)*(vc5))...
+(as*(wchar/wco2)*vp*((kg1*hmg1)/(kg1+hmg1))*(Cco2)*(vg1))+((as)*0.5*(wch
ar/wh2)*vp*((kg2*hmg2)/(kg2+hmg2))*(Ch2)*(vg2))...
+((as)*1*(wchar/wh2o)*vp*((kg3*hmg3)/(kg3+hmg3))*(Ch2ov)*(vg3));


ydot(11) =0.1*(pi*r*r)*(ll*hsg*vp*(Ts-
Tg))+(ag*kc1*Tg*Pre^0.3*Ctars^0.5*Co2*(vc1))+(ag*kc2*Tg*Cch4^0.5*Co2*(vc2
))+(ag*1*kc3*Tg*Cco*Co2^0.25*Ch2ov^0.5*(vc3))...
+(ag*2*kc4*Ch2*Co2*(vc4))+(ag*1*kg4*Cch4*Ch2ov*(vg4));

ydot(12) = 0;

ydot(13) = -(as*1*2*(wchar/wo2)*vp*((kc5*hmc5)/(kc5+hmc5))*(Co2))-
(ag*2.9*kc1*Tg*Pre^0.3*Ctars^0.5*Co2)-(ag*1.5*kc2*Tg*Cch4^0.5*Co2)-
(ag*1*kc3*Tg*Cco*Co2^0.25*Ch2ov^0.5)...
-(ag*2*kc4*Ch2*Co2);

ydot(14) = Hs-
(nchar*En_CPSO(Ts,'char')+nmoi*En_CPSO(Ts,'moi')+nbms*En_CPSO(Ts,'bms'));


ydot(15) = Hg-
(no2*En_Ch(Tg,'o2')+nn2*En_Ch(Tg,'n2')+nco*En_Ch(Tg,'co')+nco2*En_Ch(Tg,'
co2')+nh2ov*En_Ch(Tg,'h2o')+nh2*En_Ch(Tg,'h2')+nch4*En_Ch(Tg,'ch4')...
+ntars*En_CPSO(Tg,'tars'));

ydot = ydot';
```